A highly efficient intumescent polybutylene succinate: Flame retardancy and mechanistic aspects

Fei Xiao, Gaelle Fontaine, Serge Bourbigot

Version of Record: https://www.sciencedirect.com/science/article/pii/S0141391022000167
Manuscript_9b75865a2694c39cc9210a5dbe99fd8b

A highly efficient intumescent polybutylene succinate: flame retardancy and mechanistic aspects

Fei Xiao [a], Gaëlle Fontaine [a], Serge Bourbigot [a, b, *]

[a] *Univ. Lille, CNRS, INRAE, Centrale Lille, UMR 8207 - UMET - Unité Matériaux et Transformations, F-59000 Lille, France*

[b] *Institut Universitaire de France (IUF), Paris, France*

Corresponding author: serge.bourbigot@centralelille.fr

ABSTRACT

A new strategy was developed for the fabrication of intumescent flame retardant system to improve the fire performance of polybutylene succinate (PBS) based on the synergistic effect of ethylenediamine phosphate (EDAP) and melamine poly(aluminum phosphate) (MPAlP) as well as zinc borate (ZnB). Cone calorimetry results exhibited that, with only 10 wt.% total loading of additives, the peak heat release rate (pHRR) and total heat release (THR) of PBS/EDAP&MPAlP(7:3, 8%)/ZnB(2%) were significantly reduced by 63% and 13%, respectively, in comparison to PBS. Meanwhile, the fire growth rate index (FIGRA) and maximum average rate of heat emission (MARHE) were decreased by 43% and 48% respectively, and its flameout time reached up to 840 s from 493 s for neat PBS. It should be noted that solid-state MAS NMR (^{11}B, ^{13}C, ^{27}Al, and ^{31}P) technique provided information to determine chemistry in the condensed phase during combustion. It was evidenced that the combination of EDAP/MPAlP and ZnB led to the formation of a protective intumescent char embedded with highly thermally stable phosphate species (*e.g.*, boron phosphate and zinc phosphate). They improved the cohesion (crack-

free) and stability as well as the resistance of the char, thus improving the fire retardancy of PBS. Additionally, PBS/EDAP&MPAlP(7:3,8%)/ZnB(2%) showed low smoke emission and good thermal/mechanical properties, thanks to the introduction of zinc borate. As a result, this work provides a new perspective for the development of new intumescent flame retardant systems toward PBS.

Keywords: flame retardancy, polybutylene succinate, melamine poly(aluminum phosphate), ethylenediamine phosphate, zinc borate.

1. Introduction

Recently, biobased polybutylene succinate (PBS) has shown enormous potential for partially substituting petrochemical-based plastics in various application fields owing to its good processability, controlled biodegradability, and excellent thermal/mechanical properties [1-3]. Nevertheless, the inherent high flammability of PBS is one of the most pervasive problems afflicting greatly its applications where fire safety is indispensable [4-6]. Therefore, it is paramount to develop a highly efficient fire retardant system for PBS.

Up to now, numerous attempts have been made to impart fire retardancy to PBS [7-11], among which intumescent flame retardants (IFRs) are the most frequent approach to reducing the flammability of PBS [12]. Indeed, IFRs show desirable potential as promising alternative to halogen-containing and conventional flame retardants (*e.g.*, magnesium hydroxide) due to their high efficiency, low toxicity, and few smoke productions [13, 14]. A typical intumescent flame retarded PBS system comprises an acid source (*e.g.*, ammonium polyphosphate), a blowing agent (*e.g.*, melamine), and/or a carbonization agent (*e.g.*, natural fibers, pentaerythritol). To our knowledge, the most common IFR system for PBS is ammonium polyphosphate/melamine system

combined with various synergists [15-19]. However, in those formulations, relatively high loading (more than 20%, see Table 1) is essential to meet the fire safety requirements, which may cause the deterioration of mechanical properties.

Table 1. Comparison of flame retardancy of intumescent PBS formulations of this work and previous works.

Total loading	IFR system and loading	Synergist and loading	ΔpHRR	ΔTHR	Ref.
30%	MP, 30%	/	-33%	-22%	[9]
30%	APP, 30%	/	-19%	-25%	[20]
30%	APP&MEL (5:1), 23%	MHSH, 2%; ES-CD, 5%	-36%	-9%	[21]
25%	APP&MEL (5:1), 23%	MHSH, 2%	-50%	-11%	[15]
25%	APP&MEL (5:1), 23%	Urea-kaolinite, 5%	-49%	-24%	[22]
25%	APP&MEL (5:1), 20%	HAPCP-kaolinite, 5%	-49%	-18%	[23]
25%	APP&MEL (5:1), 24%	Lignin chelates, 1%	-59%	-10%	[24]
25%	APP&MEL (5:1), 22%	Lignin-MMT, 3%	-57%	-27%	[25]
21%	APP&MEL (2:1), 20%	OMMT, 1%	-67%	-49%	[18]
20%	APP&MEL (5:1), 19%	MgAlZnFe LDHs, 1%	-30%	-19%	[26]
20%	MP, 18%	Graphene, 2%	-63%	-22%	[7]
20%	APP, 15%	Sepiolite, 5%	-57%	-11%	[27]
10%	***EDAP&MPAlP (7:3), 8%***	***Zinc borate, 2%***	***-63%***	***-13%***	***This work***

Note: APP, ammonium polyphosphate; HAPCP-kaolinite, hexakis (4-aldehyde phenoxy) cyclotriphosphazene grafted kaolinite; Lignin-MMT, lignin-modified montmorillonite; MEL, melamine; MgAlZnFe-LDHs, MgAlZnFe-CO_3 layered double hydroxide; MHSH, magnesium hydroxide sulfate whisker; MP, melamine phosphate; OMMT, organically (acetyl quaternary ammonium) modified Ca-montmorillonite; Urea-kaolinite, urea-modified kaolinite; ΔPHRR, reduction of pHRR compared with neat PBS; ΔTHR, reduction of THR compared with neat PBS.

In our previous work [28], a series of intumescent PBS formulations were developed based on ethylenediamine phosphate (EDAP) and different co-additives. Unfortunately, all those formulations exhibited relatively high peak heat release rates (pHRR) during combustion. In order to further improve the char quality and to enhance the flame retardancy of intumescent PBS systems, in this work, a highly-efficient ternary IFR system was designed to flame retard PBS by introducing ethylenediamine phosphate (EDAP), melamine poly(aluminum phosphate) (MPAlP), and zinc borate into PBS. There is evidence that the appropriate combination of two or more additives may result in improved flame retardancy through synergistic interactions due to their

different main mode of action [29]. EDAP is a commercially available non-halogenated intumescent flame retardant prepared by phosphoric acid and ethylenediamine, which can simultaneously play the roles of acid source (19.5% phosphorus) and blowing agent (17.7% nitrogen) during the combustion [30]. Therefore, it is widely used in various polyolefins to promote both charring and the formation of highly crosslinked phospho-carbonaceous structures [31]. MPAlP combines the benefits of nitrogen (melamine) and phosphorus-based flame retardants, and it employs multidimensional modes of flame retardant actions in the gas and condensed phases [32]. On the one hand, melamine derivatives decompose endothermically, releasing inert nitrogen-containing gases (blowing) and generating melamine homologues (melam, melem, and melon) which can improve the thermal/fire resistance of char [33]. On the other hand, phosphorus-containing decomposition products can promote the formation of insulating char on the surface. Moreover, it has been widely applied to enhance the fire retardancy of glass fiber reinforced polyamide 6,6 and epoxy resin [32-36]. Importantly, the external heat flux and internal pressure caused by the evolved products may lead to the formation of cracks in the intumescent char, thereby decreasing the fire-retardant efficiency of carbonaceous barrier. Based on our previous works [28, 37, 38], zinc borate shows significant synergistic interactions with phosphate-based flame retardants. It can efficiently enhance the cohesion and heat resistance of residual char by forming a protective vitreous layer (mainly B_2O_3) on the burning material surface [39, 40]. In conclusion, the comprehensive performances of PBS and its composites, including thermal stability, flame retardancy, combustion behavior, smoke release, and mechanical properties, were evaluated in detail, and the flame retardant mechanisms of action of intumescent PBS in condensed phase and in gas phase were also investigated using various techniques.

2. Experimental

2.1 Materials

Biobased polybutylene succinate (Bionolle™ 1001 MD, melting point: 114 ºC, melt flow rate: 1-3 g/10 min) was procured from Showa Denko, Japan. Melamine poly(aluminum phosphate) (MPAlP [33]) was provided by Caterna-Floridienne Chemie, France, ethylenediamine phosphate (EDAP, $C_2H_{11}N_2O_4P$) was purchased from CHEMOS GmbH, Germany, and zinc borate (Firebrake® ZB, $2ZnO{\cdot}3B_2O_3{\cdot}3.5H_2O$, median particle size: 9 microns) was supplied by US Borax, USA. All the materials were dried in oven at 80 ºC overnight before use.

2.2 Preparation of PBS composites

The detailed formulations for PBS and its composites are presented in Table 2. In all PBS formulations, the filler loading was kept constant at 10 wt.%. All PBS formulations were prepared by compounding biobased PBS and flame retardant additives (MPAlP, EDAP, and zinc borate) in a torque mixer at 140 ºC for 15 min, and the detailed preparation process has been reported in our previous work [28].

Table 2. Formulation of PBS composites.

Sample	**Composition (wt.%)**			
	PBS	Ethylenediamine phosphate	Melamine poly(aluminum phosphate)	Zinc borate
PBS	100	/	/	/
PBS/MPAlP	90	/	10	/
PBS/EDAP	90	10	/	/
PBS/EDAP&MPAlP(9:1)	90	9	1	/
PBS/EDAP&MPAlP(8:2)	90	8	2	/
PBS/EDAP&MPAlP(7:3)	90	7	3	/
PBS/EDAP&MPAlP(5:5)	90	5	5	/
PBS/EDAP&MPAlP(2:8)	90	2	8	/
PBS/EDAP&MPAlP(7:3, 9%)/ZnB(1%)	90	6.3	2.7	1
PBS/EDAP&MPAlP(7:3, 8%)/ZnB(2%)	90	5.6	2.4	2
PBS/EDAP&MPAlP(7:3, 7%)/ZnB(3%)	90	4.9	2.1	3

2.3 Characterizations

2.3.1 Fire and smoke tests

On the basis of the standards of ASTM E 906, forced flaming combustion test of PBS and of its composites was performed using a Fire Testing Technology (FTT, UK) Mass Loss Cone Calorimeter (MLCC). The heat release rate (HRR) of samples was measured using the thermopile in the chimney. The samples with a size of 100 mm × 100 mm × 3 mm were exposed to a conical heater (heat flux of 35 kW/m^2) with a distance of 25 mm, corresponds to a developing fire scenario [41]. The smoke release behavior was assessed by analyzing the opacity of smoke emitted from the top of the chimney during the MLCC test, according to the method of previous work [28, 42]. Moreover, MLCC was also coupled with a Fourier Transform InfraRed device (Antaris™ IGS) to quantitatively analyze the real-time composition and content of evolved products during combustion, such as water, carbon dioxide, and carbon monoxide [43].

2.3.2 Solid state NMR analysis

^{11}B magic angle spinning (MAS) nuclear magnetic resonance (NMR) measurements were performed on a Bruker Avance III 800 spectrometer (18.8 T) at a frequency of 256.6 MHz with a recycle delay of 2 s and a scans number of 512. The 3.2 mm probe head was operated at a spinning frequency of 20 kHz. ^{13}C NMR experiments were conducted on a Bruker Avance II 400 spectrometer (9.4 T) operating at 100.6 MHz with a probe head of 4 mm, a recycle delay of 5 s. The ^{1}H-^{13}C cross-polarization (CP) NMR spectra were carried out at a spinning frequency of 12.5 kHz with 1024 scans. ^{27}Al MAS NMR measurements were carried out on a Bruker Avance II 400 spectrometer (9.4 T) with a probe head of 3.2 mm, a recycle delay of 1 s, operating at a spinning frequency of 20 kHz. The spectra were acquired as a result of 1024 scans. ^{31}P NMR experiments were performed on the same spectrometer (9.4 T) as above operating at 162 MHz. The analysis

was carried out with a 4 mm probe head with ^{1}H decoupling (DD) with 120 s recycle delay. The ^{31}P NMR spectra were recorded with 16 scans and a spinning frequency of 12.5 kHz.

2.3.3 TGA and TGA-FTIR

Thermogravimetric analysis (TGA) was carried out on a TA Instrument TGA Q5000IR under nitrogen environment. Samples were heated from 40 ºC to 800 ºC with a heating rate of 10 ºC/min and a continuous purge flow of 50 mL/min. Weight difference curves were calculated based on the difference between experimental and calculated TGA curves of the mixture. The calculation method was described in detail in our previous work [44]. Moreover, The TA Instrument Q5000 IR was coupled with Thermo Scientific Nicolet iS10 FT-IR spectrometer by a heated transfer line (190 ºC) to measure the TGA-FTIR spectra of samples. The real-time FTIR spectra were collected every 10 s with 8 scans.

2.3.4 Mechanical properties

The tensile test was performed on an Instron 4466 compression tension tensile tester (10KN, USA) to study the mechanical properties of PBS and its composites. Samples with a gauge length of 80 mm (127 mm total length) and a cross-section of 12.7 mm × 1.7 mm, were tested with a constant speed of 10 mm/min. At least five specimens were measured for each formulation.

3. Results and discussion

3.1 Fire performance of PBS composites

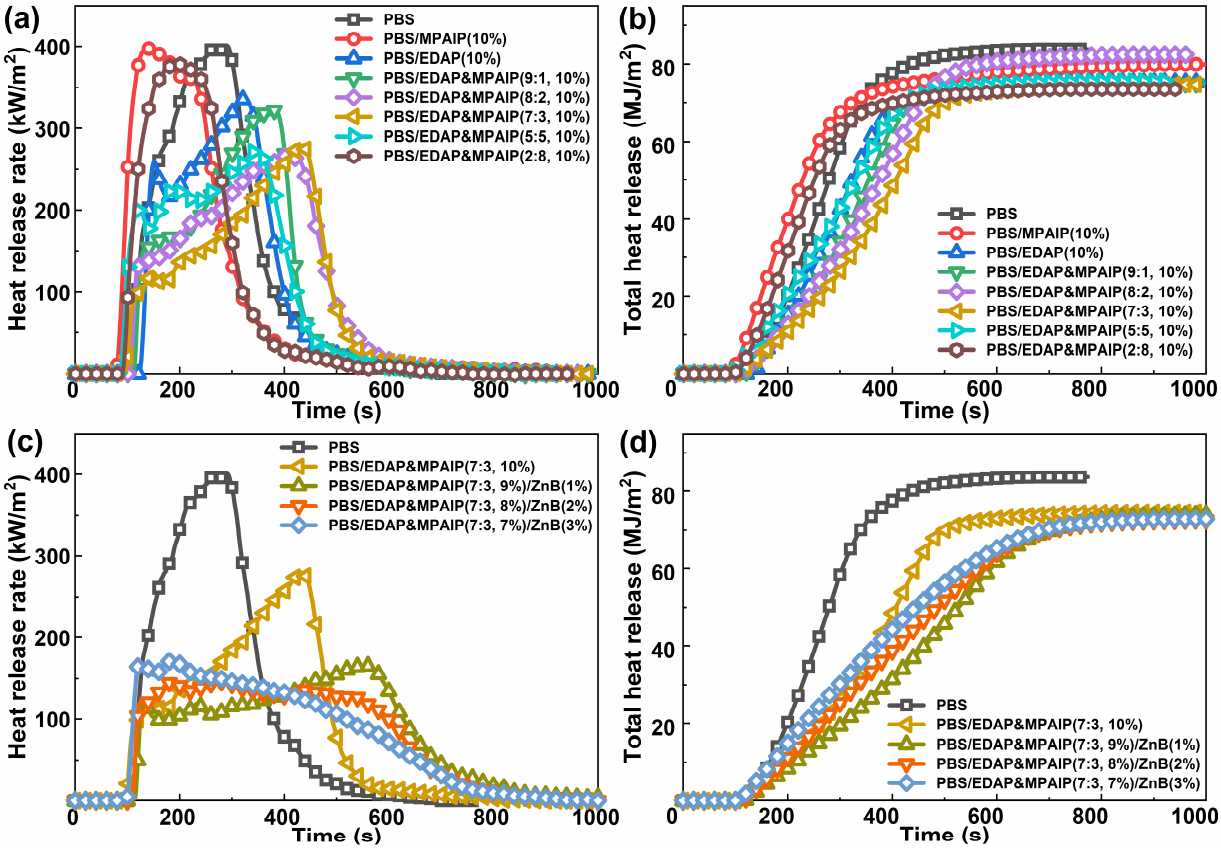

Figure 1. (a, c) HRR and (b, d) THR curves of PBS and its composites at a heat flux of 35 kW/m^2.

Table 3. MLCC data of PBS and its composites (35 kW/m^2).

Sample	TTI (s)	$t_{Flameout}$ (s)	pHRR (kW/m^2)	THR (MJ/m^2)	FIGRA (kW/(m^{2}s))	MARHE (kW/m^2)	FRI
PBS	109	493	401	83.7	1.69	206	/
PBS/MPAlP	84	430	399	77.1	3.11	231	0.84
PBS/EDAP[28]	125	476	336	74.6	1.72	172	1.54
PBS/EDAP&MPAlP(9:1)	113	462	322 (-4%)	74.5 (0%)	1.16 (-33%)	163 (-5%)	1.45
PBS/EDAP&MPAlP(8:2)	106	558	267 (-21%)	82.0 (10%)	1.08 (-37%)	155 (-10%)	1.49
PBS/EDAP&MPAlP(7:3)	99	544	280 (-17%)	74.4 (0%)	0.83 (-52%)	141 (-18%)	1.46
PBS/EDAP&MPAlP(5:5)	87	512	271 (-19%)	75.3 (-1%)	1.69 (-2%)	167 (-3%)	1.31

PBS/EDAP&MPAlP(2:8)	92	389	379 (13%)	72.7 (-3%)	2.31 (+34%)	210 (+22%)	1.03
PBS/EDAP&MPAlP(7:3)	99	544	280	74.4	0.83	141	1.46
PBS/EDAP&MPAlP(7:3, 9%)/ZnB(1%)	115	955	163 (-42%)	74.3 (0%)	0.91 (10%)	103 (-27%)	2.92
PBS/EDAP&MPAlP(7:3, 8%)/ZnB(2%)	110	840	149 (-47%)	72.7 (-2%)	0.97 (17%)	106 (-25%)	3.13
PBS/EDAP&MPAlP(7:3, 7%)/ZnB(3%)	101	791	171 (-39%)	72.9 (-2%)	1.38 (66%)	113 (-20%)	2.49

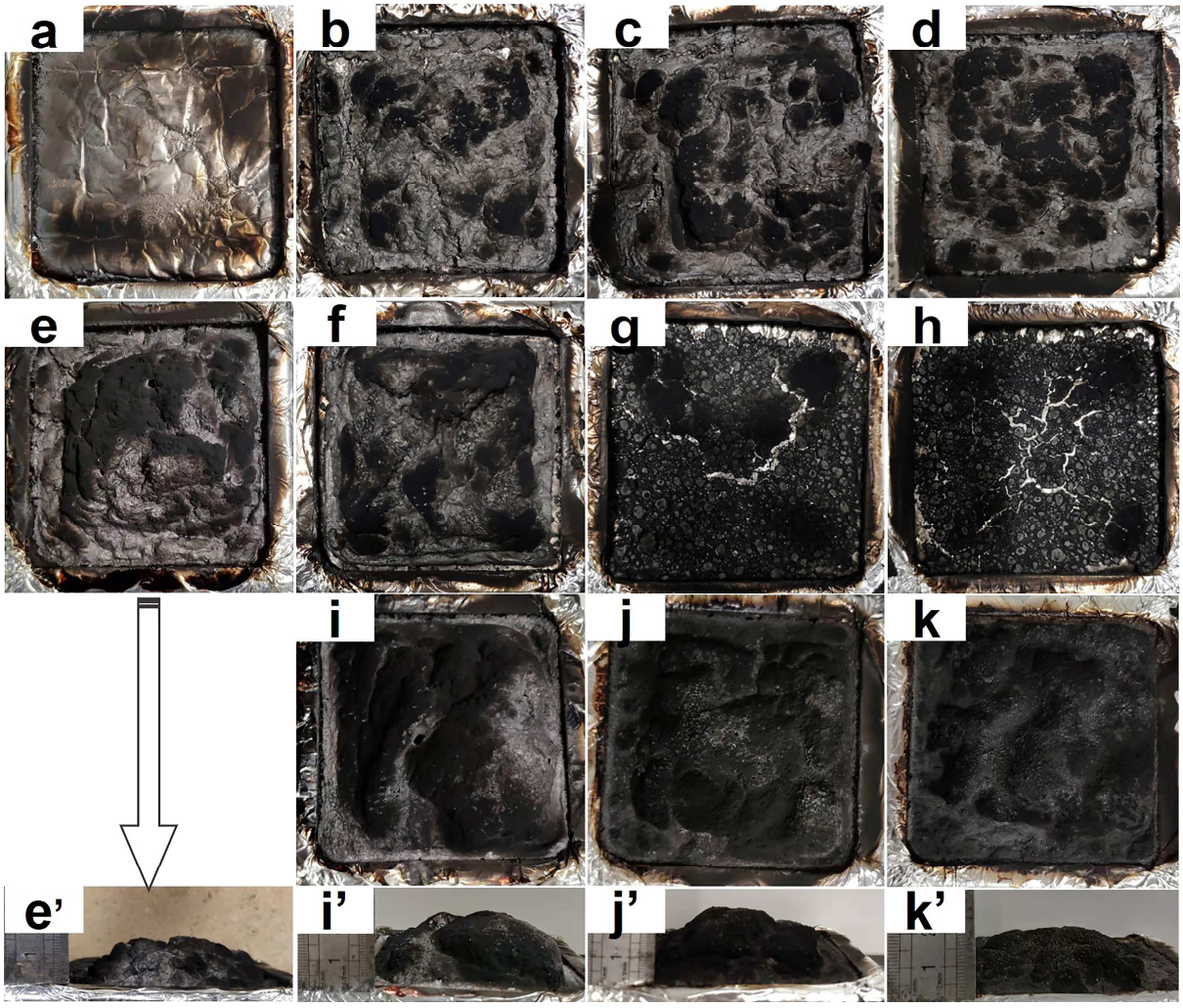

Figure 2. Morphology of char residues of (a) PBS, (b) PBS/EDAP, (c) PBS/EDAP&MPAlP(9:1), (d,) PBS/EDAP&MPAlP(8:2), (e, e') PBS/EDAP&MPAlP (7:3), (f) PBS/EDAP&MPAlP(5:5), (g) PBS/EDAP&MPAlP(2:8), (h) PBS/MPAlP, (i, i') PBS/EDAP&MPAlP(7:3, 9%)/ZnB(1%), (j, j') PBS/EDAP&MPAlP(7:3, 8%)/ZnB(2%), (k, k') PBS/EDAP&MPAlP(7:3, 7%)/ZnB(3%) after MLCC test.

3.1.1 Effect of the mass ratio of EDAP and MPAlP

The combustion behaviors of PBS and its composites were investigated in a forced combustion condition provided by MLCC test. The heat release rate (HRR) and total heat release (THR) curves of PBS and its composites are presented in Figure 1, the correlative characteristic parameters are summarized in Table 3. Moreover, the morphology of residues for PBS and its composites after MLCC test are shown in Figure 2.

The HRR curve of neat PBS shows a typical shape for non-charring polymeric materials (Figure 1a), it burns rapidly with a high pHRR of 401 kW/m^2 and a THR of 83.7 MJ/m^2, without residue formation. Addition of 10 wt.% EDAP limitedly reduces the pHRR and THR by 16% (336 kW/m^2) and 11% (74.6 MJ/m^2), respectively, compared to that of neat PBS. The fire behavior of PBS/EDAP is still poor due to the formation of island-like residue with numerous cracks (Figure 2b). This limited action in the condensed phase of PBS/EDAP is due to the poor intumescence and cohesion of char [20]. Similarly, the incorporation of 10 wt.% MPAlP alone into PBS does not decrease the pHRR value, but also promotes the faster decomposition of PBS/MPAlP composite (pHRR is reached at shorter time as compared to PBS). It is observed that the incorporation of MPAlP leads to the formation of fragmented residue (Figure 2h), which fails to protect the underneath polymeric matrix. So, MPAlP or EDAP alone are not sufficient to reach acceptable fire performance. Compared to PBS/EDAP, the partial substitution of EDAP by 1 wt.% MPAlP visibly reduces the initial peak in HRR of PBS/EDAP&MPAlP(9:1). However, the pHRR is still as high as 322 kW/m^2, which is similar to that of PBS/EDAP (4% reduction). When EDAP and MPAlP are incorporated in PBS at a ratio of 8:2, the initial peak in HRR of PBS/EDAP&MPAlP(8:2) decreases further, and its pHRR decreases by 21% (267 kW/m^2) in

comparison to PBS/EDAP. The residues of PBS/EDAP&MPAlP (9:1) and PBS/EDAP&MPAlP (8:2) show relatively complete char layer (Figure 2c-d), however, visible cracks are still observed.

Furthermore, it is clear that the combination of EDAP and MPAlP(7:3) prolongs the time to pHRR from 322s for PBS/EDAP to 427s, meanwhile, the pHRR is decreased to 280 kW/m^2 (-17%), indicating the synergistic effect between EDAP and MPAlP (7:3). In contrast to PBS/EDAP and PBS/MPAlP, visual observation shows that a relatively continuous intumescent char layer is formed for PBS/EDAP&MPAlP(7:3) (Figure 2e-e'), thanks to the construction of intumescent system where EDAP acts as acid source and MPAlP mainly acts as blowing agent. The initial peak of HRR of PBS/EDAP&MPAlP(7:3) appears rapidly and the formation of protective char at early stage is observed. However, the HRR then increases gradually until pHRR, indicating the barrier effect of the formed char is not strong enough. Further reducing the EDAP&MPAlP ratio to 5:5 or 2:8 results in the increase in initial HRR peak (Figure 1a), and at the same time the pHRR value began to increase. Note that PBS/EDAP&MPAlP(5:5) forms a relatively complete residual char (Figure 2f), whereas a fragmented char is found for PBS/EDAP&MPAlP(2:8) (Figure 2f) which is similar to that of PBS/MPAlP.

Fire growth rate index (FIGRA) and maximum average rate of heat emission (MARHE), two important fire safety engineering parameters, were applied to assess the fire growth and spread rates of material [45]. Generally, lower FIGRA value means slower flame spread potential and more time to escape from the fire; and lower MARHE represents the worse ability to support flame spreading to other objects. The FIGRA and MARHE of PBS are 1.69 kW/(m^{2}s) and 206 kW/m^2, whereas PBS/MPAlP shows higher FIGRA (3.11 kW/(m^{2}s)) and MARHE (231 kW/m^2), suggesting that the incorporation of 10 wt.% MPAlP alone deteriorates the fire performance of PBS. For PBS/EDAP, FIGRA is similar to that of neat PBS, and its MARHE decreases by 17%.

This means that the addition of 10 wt.% EDAP shows limited effect on fire properties of PBS. Interestingly, compared to PBS/EDAP, the combination of EDAP and MPAlP from 9:1 to 7:3 results in further reduction in FIGRA (1.16, 1.08, and 0.83 kW/(m^2s), respectively) and MARHE (163, 155, and 141 kW/m^2, respectively) of PBS. Among them, PBS/EDAP&MPAlP(7:3) presents lowest FIGURE and MARHE values, demonstrating the improvement of the fire growth and spread performance. Flame retardancy index (FRI) was introduced to evaluate the flame retardancy of PBS composites [46]. On the contrary to FIGRA and MARHE, a higher FRI value represents the better flame retardancy of composite. The FRI value of PBS/MPAlP is only 0.84 (<1), indicating a bad flame retardancy effect. For PBS/EDAP (1.54), the incorporation of 10 wt.% EDAP enhances the flame retardancy of PBS to some extent. Unfortunately, it can be seen that, compared to PBS/EDAP, the flame retardancy of PBS composites is not improved when combined EDAP and MPAlP from 9:1 to 7:3 in terms of FRI.

3.3.2 Effect of the loading of zinc borate

Even though there is a synergistic effect between EDAP and MPAlP on flame retardancy and intumescence of PBS, the flame retardant efficiencies of PBS/EDAP&MPAlP composites are still low, which is reflected in the limited reductions in pHRR, FIGRA, and MARHE. To further improve the intumescence and fire retardancy of PBS, zinc borate was incorporated as potential synergist to PBS (see Figure 1c-d, Table 3), and the EDAP&MPAlP(7:3) system was chosen as intumescent system based on the above investigations.

With the addition of zinc borate from 1 wt.% to 3 wt.%, the pHRR values of PBS/EDAP&MPAlP(7:3, 9%)/ZnB(1%), PBS/EDAP&MPAlP(7:3, 8%)/ZnB(2%), and PBS/EDAP&MPAlP(7:3, 7%)/ZnB(3%) are decreased to 163, 149, and 171 kW/m^2 respectively, showing 42%, 47%, and 39% reductions in comparison to that of PBS/EDAP&MPAlP(7:3). It

implies the synergistic effect between zinc borate and EDAP&MPAlP(7:3) in improving the fire retardancy of PBS. The THR values for all PBS/EDAP&MPAlP/ZnB formulations (1% - 3% ZnB loadings) show similar results to that of PBS/EDAP&MPAlP(7:3). Compared to PBS/EDAP&MPAlP(7:3), the incorporation of zinc borate from 1% to 3% significantly reduces the MARHE values by 27%, 25%, and 20% respectively. It is to be noted that PBS/EDAP&MPAlP(7:3, 8%)/ZnB(2%) exhibits the highest FRI value (3.13) and the lowest pHRR value, revealing that 2 wt.% loading of zinc borate is the optimal ratio to improve the flame retardancy of PBS.

Regarding the residual chars of zinc borate-containing PBS composites, visual observation (Figure 2i-k) suggests that zinc borate noticeably modifies the fire and charring behaviors of PBS composites, resulting in the formation of a compact and crack-free char layer protecting the underneath polymer matrix with different level of efficiency. This phenomenon implies an additional mechanism of action occurred in the condensed phase with the addition of zinc borate. The formed char layer acts as a protective physical barrier, which limits the heat and mass transfer between condensed and gas phases. Moreover, the char swelling degree (in terms of the height of char) of PBS composites with 1 or 2 wt.% zinc borate loading is higher than that of 3 wt.% loading, indicating that a relatively low loading of zinc borate is more efficient to promote the expansion of char when the total loading is constant (10 wt.%).

According to the above analysis, in the following, we only focus our work on the flame retarded formulations of PBS/EDAP&MPAlP(7:3) and PBS/EDAP&MPAlP(7:3,8%)/ZnB(2%) (they are hereafter called *PBS/EDAP&MPAlP* and *PBS/EDAP&MPAlP/ZnB*).

3.2 Smoke release behavior and combustion product analysis

3.2.1 Smoke release behavior

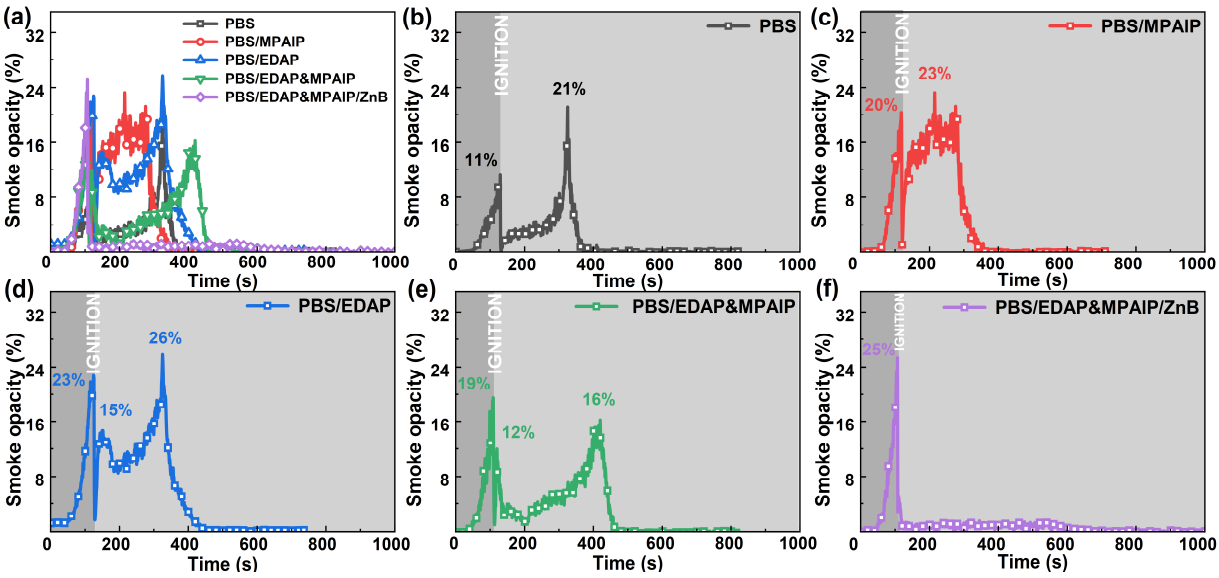

Figure 3. Smoke opacity of (a) PBS and its composites during MLCC test: (b) PBS, (c) PBS/MPAlP, (d) PBS/EDAP, (e) PBS/EDAP&MPAlP, and (f) PBS/EDAP&MPAlP/ZnB (Dark gray area: before ignition, light gray area: after ignition).

Smoke is a dominant hazard factor in fires, which may cause heavy casualties due to the toxicity and low visibility. Generally, a low smoke opacity corresponds to the high visibility, which raises the chance to escape from a fire [47]. The smoke release behavior of PBS and its composites was investigated by studying the smoke opacity of PBS and its composites during the MLCC test (Figure 3).

Before ignition, the peak smoke opacity of PBS/MPAlP and PBS/EDAP reaches 20% and 23% respectively, which is approximately twice the peak value of PBS (11%). A reasonable explanation is that the incorporation of MPAlP and EDAP leads to the uncomplete combustion of materials thus increasing the smoke opacity. Compared with PBS/MPAlP and PBS/EDAP, the combination of MPAlP and EDAP results in a slight reduction in smoke opacity with a peak of

19%. For PBS/EDAP&MPAlP/ZnB, a higher peak appears before ignition with a smoke opacity of 25%, which is ascribed to the incorporation of zinc borate.

For all formulations, the smoke opacity values sharply drop to almost zero when ignition occurs, this is due to the combustion and the consumption of evolved pyrolysis products. After ignition, the opacity of smoke for PBS gradually increases and shows a sharp peak of 21%, demonstrating the low smoke release of neat PBS during combustion [24]. For PBS/MPAlP, the opacity of the smoke rises quickly after ignition and presents an intensity broad zone in around 150 to 250 s with a peak smoke opacity of 23% (Figure 3c). This indicates that the incorporation of 10 wt.% MPAlP alone to PBS promotes the production of smoke. The smoke opacity of PBS/EDAP increases to 15% sharply and then reduces, corresponding to the formation of char. However, with the time increases, the opacity of the smoke of PBS/EDAP climbs up to 26% at 325s, which means that the addition of EDAP char cannot effectively decrease the release of smoke. The smoke opacity of PBS/EDAP&MPAlP shows a sharp peak (12%) after ignition, subsequently, it gradually increases and reaches a peak of 16% at 415 s. It is assigned to the synergy between MPAlP and EDAP reducing the smoke emission of PBS. Interestingly, when EDAP&MPAlP is partially replaced by 2 wt.% zinc borate, the smoke opacity of PBS/EDAP&MPAlP/ZnB dramatically drops to 0 after ignition and then maintains at a very low level (Figure 3f). The results imply that the combination of EDAP&MPAlP and zinc borate permits to produce PBS with low smoke emission during combustion.

3.2.2 MLCC-FTIR analysis

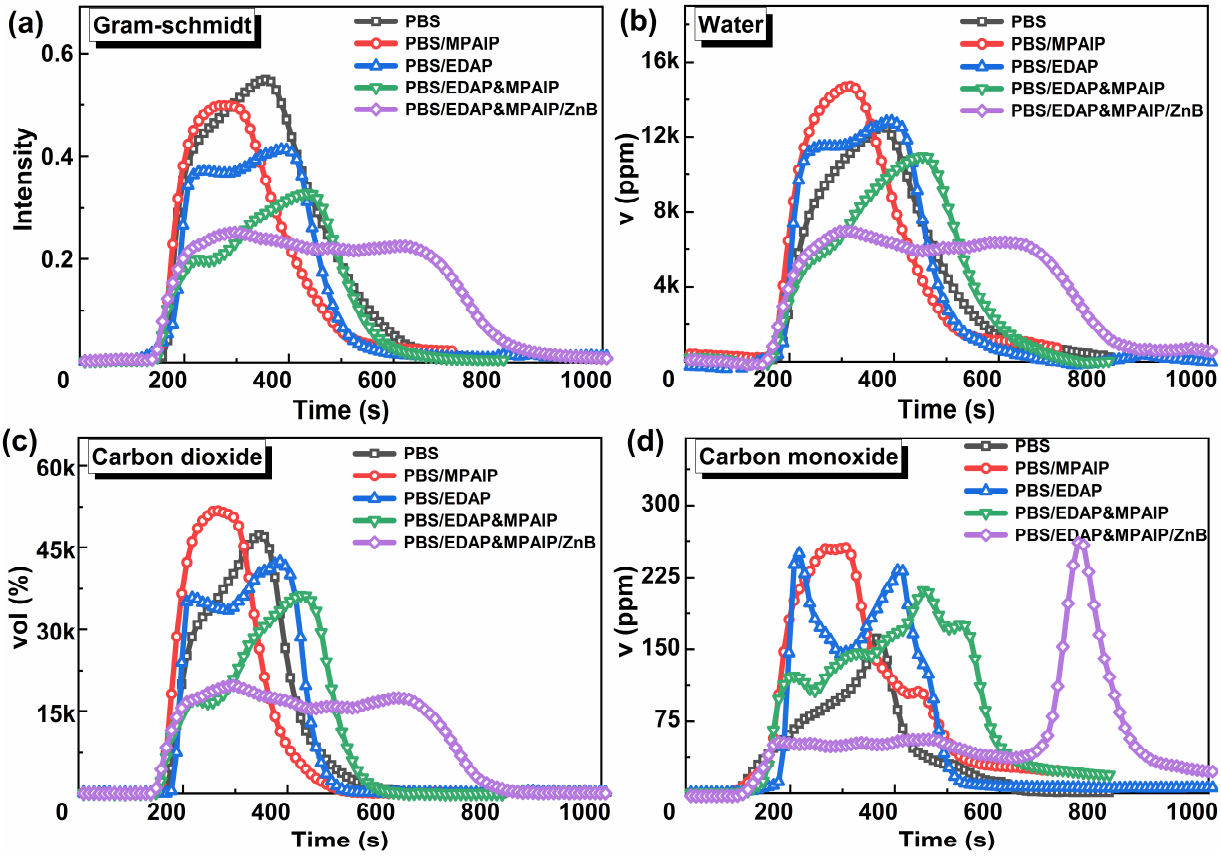

Figure 4. (a) Gram-Schmidt, (b) water, (c) carbon dioxide, and (d) carbon monoxide evolutions for PBS and its composites during MLCC test.

FTIR was coupled with MLCC to quantitatively analyze the composition and content of the evolved gases, such as water, carbon dioxide, carbon monoxide, during MLCC test [48]. As presented in Figure 4a, Gram-Schmidt curves describe FTIR absorption intensity of evolved gases (mainly water and carbon dioxide) during combustion process, which shows similar shapes as the heat release curves.

The evolution of water and carbon dioxide for PBS climbs rapidly to the peaks of 12546 ppm at 375s and 47308 ppm at 346 s, respectively (Figure 4b-c). This is due to the complete combustion of the PBS after ignition. Besides, carbon monoxide is detected before ignition, which may be

derived from the thermal-oxidative decomposition of neat PBS. The carbon monoxide emission of PBS gradually increases after ignition and reaches a peak of 161 ppm at 366 s.

It is worth noting that PBS/MPAlP shows intense release peaks of water (14710 ppm), carbon dioxide (51761 ppm), and carbon monoxide (254 ppm). This suggests that the addition of 10 wt.% MPAlP dramatically changes the decomposition rate and ultimately accelerates the combustion of composite. Similarly, these phenomena are also observed on PBS/EDAP composites. Compared to PBS, the water (10958 ppm) and carbon dioxide (36286 ppm) emission peaks for PBS/EDAP&MPAlP are reduced by 13% and 23% respectively, meanwhile, the peaks appear later (455 s and 425 s). This is due to the formed char which permits a certain flame shielding effect limiting the release of flammable products and hence, delaying the combustion process. Moreover, compared to PBS, the carbon monoxide emissions of PBS/MPAlP, PBS/EDAP, and PBS/EDAP&MPAlP remain at a relatively high level during the combustion process (peaks of 254, 250, and 211 ppm, respectively, Figure 4d), corresponding to the occurrence of incomplete combustion. These results indicate that a possible flame retardant mechanism of action may exist in the gas phase when incorporating MPAlP and/or EDAP into PBS [49].

Interestingly, the water, carbon dioxide, and carbon monoxide emission curves of PBS/EDAP&MPAlP/ZnB exhibit low emission intensity during combustion. This phenomenon is ascribed to the significant barrier effect of the protective intumescent char inhibiting the release of pyrolysis products into gas phase, thereby reducing the intensity of combustion. Also, a sharp emission peak of carbon monoxide (261 ppm) is detected at around 751 s (Figure 4d), which should be due to the smoldering of the underneath matrix.

3.3 Condensed phase analysis

3.3.1 Morphology of char residues during MLCC test

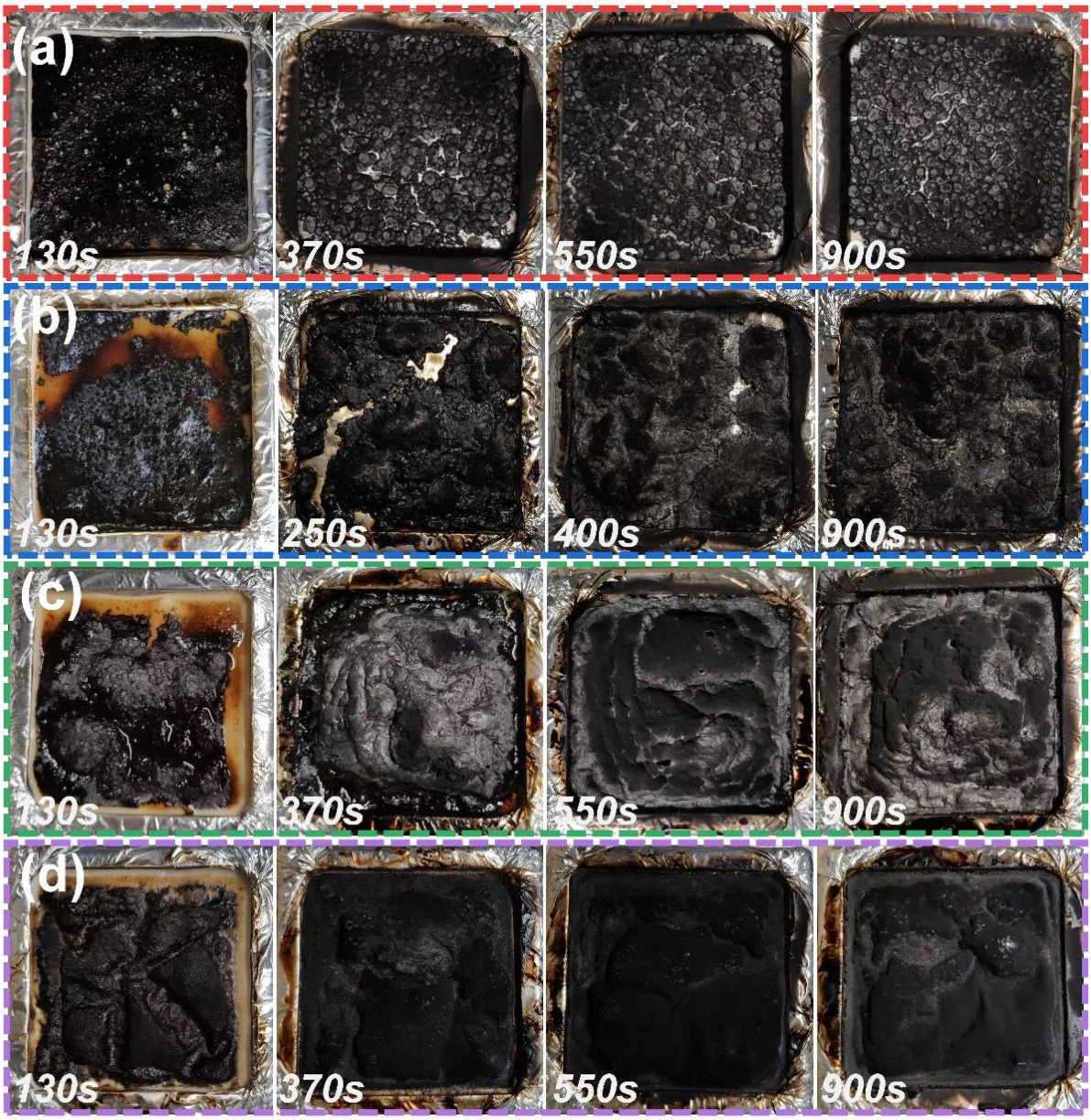

Figure 5. Char residues of (a)PBS/MPAlP, (b) PBS/EDAP, (c) PBS/EDAP&MPAlP, and (d) PBS/EDAP&MPAlP/ZnB at different times during MLCC test.

The formation and evolution of char of the PBS composites at different times in the MLCC test were studied (Figure 5) based on four parallel tests. PBS/MPAlP fails to form a char layer at the surface of the composite in the early stage of burning (130 s, Figure 5a). As the testing time increases, residue fragments can be distinguished (visual observation). On the other hand, incorporation of 10 wt.% EDAP in PBS promotes the formation of a discontinuous and collapsed char (Figure 5b), which also cannot entirely cover the surface of the sample during burning, thus resulting in the poor flame retardant efficiency. Note that the combination of MPAlP and EDAP leads to the formation of an intumescent char during the combustion (Figure 5c). This is interpreted by the synergistic effect between MPAlP and EDAP, which is attributed to the construction of the intumescent system, where EDAP acts as a strong acid source and MPAlP acts as blowing agent and acid source. As discussed earlier, the formed char may act as a physical barrier protecting underneath polymeric matrix. However, this intumescent system shows limited shielding performance due to the existence of holes and cracks on the surface of the char.

Interestingly, the presence of zinc borate visibly modifies the char morphology of PBS/EDAP&MPAlP/ZnB (Figure 5d). A flexible and crack-free intumescent char layer is observed in the early stages of burning (130 s). The formed protective intumescent char expands continuously during the burning and finally completely covers the surface of the composite, thereby leading to outstanding fire performance. This process was also identified by the fire behavior during MLCC test (Figure 6). PBS burns violently after ignition, whereas PBS/EDAP&MPAlP/ZnB forms quickly an intumescent char (130 s). This intumescent char acts as a protective fire barrier retarding mass and heat transfer between condensed and gas phase and protecting the underneath matrix from direct exposure to fire and heat flux.

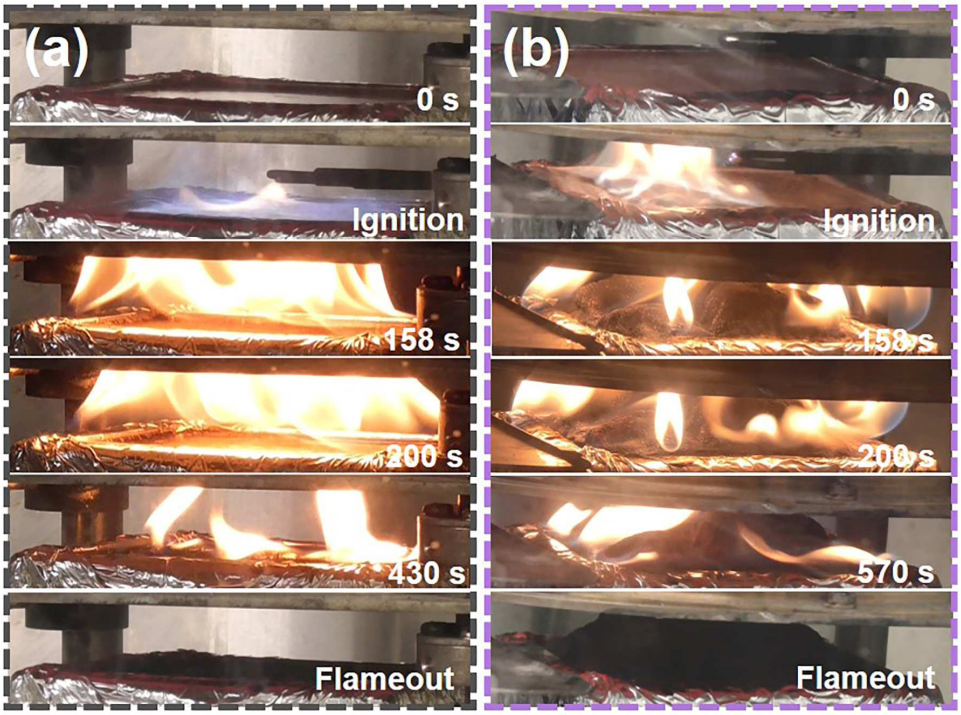

Figure 6. Fire behavior of (a) PBS and (b) PBS/EDAP&MPAlP/ZnB during MLCC test.

The surface residues obtained at different times during MLCC test were collected and further investigated by solid state NMR to understand the interaction between additives and PBS matrix in the condensed phase and to gain insight into the flame retardant mechanisms.

3.3.2 Solid-state NMR analysis

Since the thermal stability and flame retardancy of residue depends on its chemical structure, solid-state NMR was measured to investigate the evolution of specific chemical species by analyzing the intermediate species of char formed at different times during burning. By observing the selected nucleus (here, ^{11}B, ^{13}C, ^{27}Al, and ^{31}P) and its surrounding, one can gain insight into the reaction-to-fire (reactivity) of PBS composites.

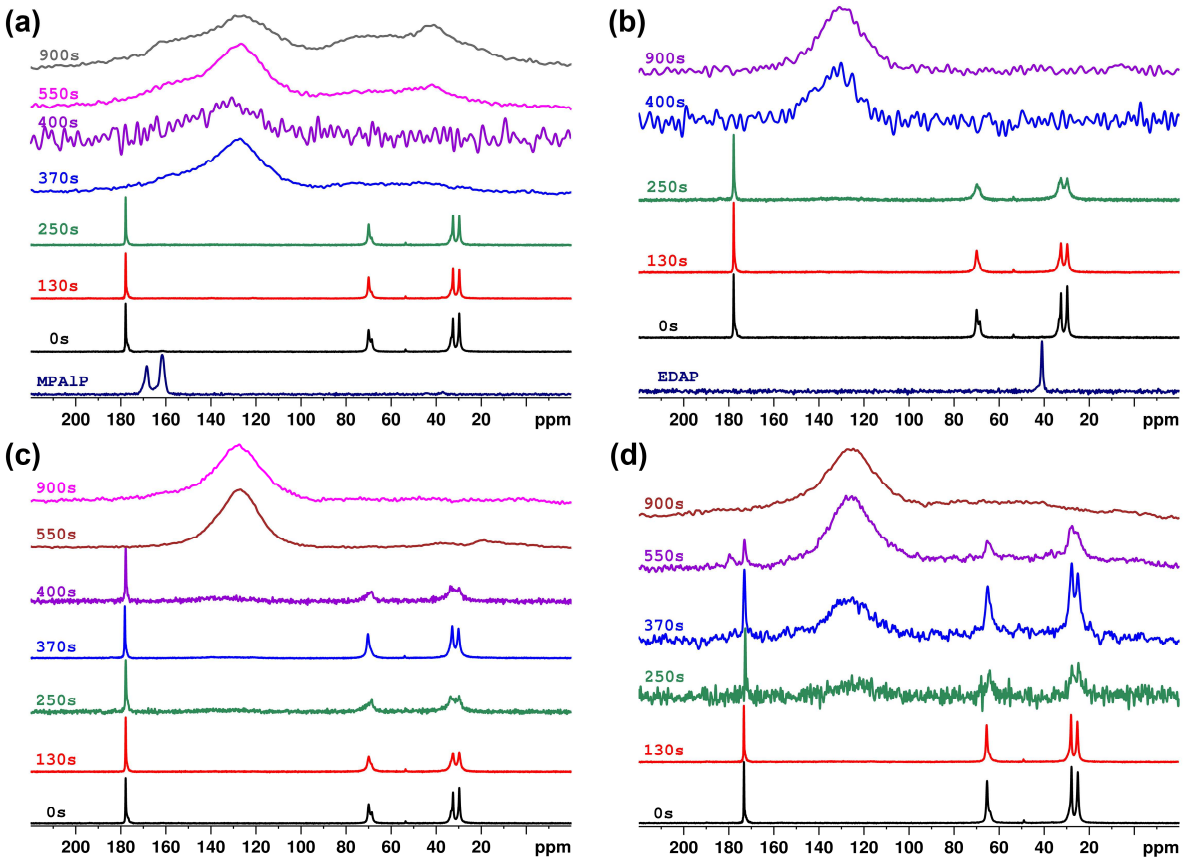

Figure 7. ^{13}C CP-MAS ssNMR spectra of (a) PBS/MPAlP, (b) PBS/EDAP, (c) PBS/EDAP&MPAlP, and (d) PBS/EDAP&MPAlP/ZnB.

Figure 7 presents the ^{13}C CP-MAS NMR spectra of additives and PBS composites. It can be seen that MPAlP shows two bands at 168.4 and 161.6 ppm, which are assigned to the carbon atoms of the triazine ring of melamine (two tautomeric forms) [34]. The spectrum of EDAP exhibits a single peak at 41 ppm, ascribing to the carbon atoms of ethylene chain. Before the test (0s), all the ^{13}C spectra of PBS composites show four resonance bands corresponding to the carbon atoms of the PBS chain [50] at around 178 ppm (-<u>C</u>O-CH$_2$-CH$_2$-<u>C</u>O-), 70 ppm (-O-<u>C</u>H$_2$-CH$_2$-CH$_2$-<u>C</u>H$_2$-O-), 33 ppm (-CO-<u>C</u>H$_2$-<u>C</u>H$_2$-CO-), and 30 ppm (-O-CH$_2$-<u>C</u>H$_2$-<u>C</u>H$_2$-CH$_2$-O-). When incorporating 10 wt.% MPAlP to PBS, the ^{13}C spectra of PBS/MPAlP (from 0 s to 250 s) present signals that corresponds to the resonance bands of PBS whereas signals from MPAlP cannot be distinguished.

A broad band centered at around 130 ppm is detected when the burning time exceeds 370 s (Figure 7a). The result indicates the formation of large sp^2 hybridized polyaromatic structure (char) [37]. Similarly, a broad band is also observed at around 130 ppm for PBS/EDAP when time exceeds 400s (Figure 7b).

In the case of PBS/EDAP&MPAlP, the characteristic signals of PBS are still distinguished at 400 s (Figure 7c), revealing the improved thermal stabilization of PBS when incorporating MPAlP and EDAP together. Interestingly, a broad band centered at around 130 ppm is observed at 250 s for PBS/EDAP&MPAlP/ZnB, indicating that zinc borate promotes charring in the early stage of combustion. It makes sense because visual observation (see Figure 5d and Figure 6b) shows the intumescence of the material, which avoids the complete decomposition of PBS. Besides, the formed intumescent char 'traps' aliphatic/polymeric chains in the char, limiting the release of flammable volatiles (less fuel) to the flame. Moreover, the characteristic bands of PBS are still found at 550 s, which may be ascribed to the formation of a thermally stable char protecting the PBS. The result shows that the addition of zinc borate improves the thermal stability of char at high temperatures, which is consistent with the previous conclusion.

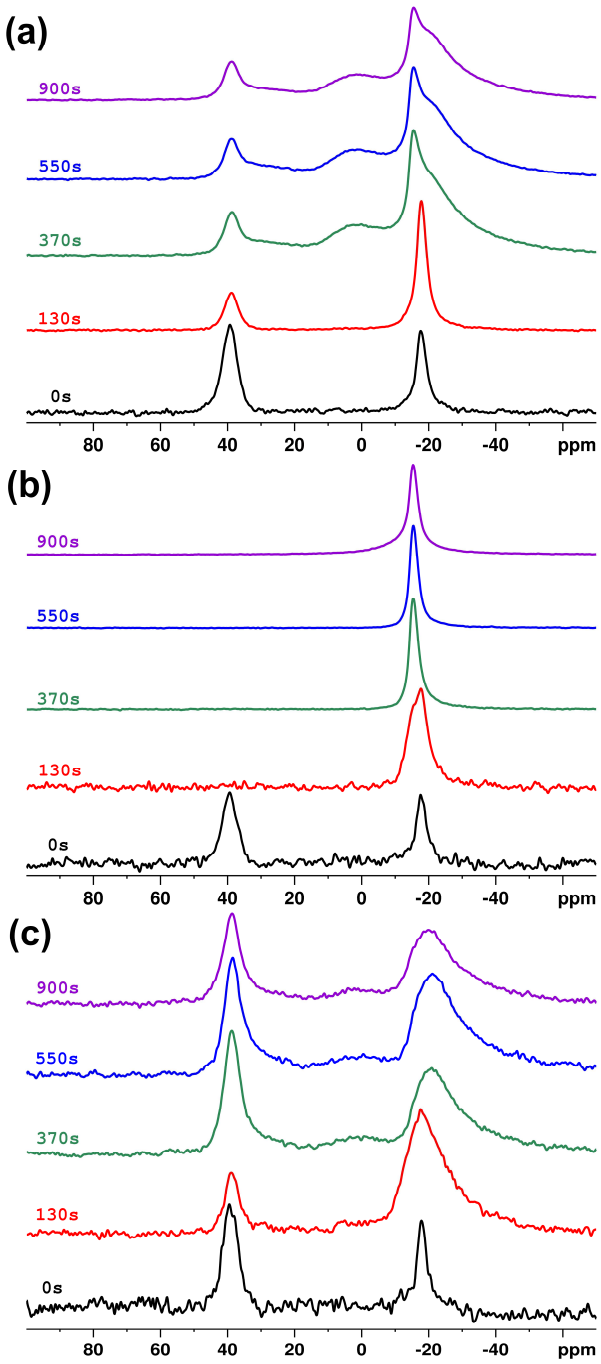

Figure 8. ^{27}Al MAS ssNMR spectra of (a) PBS/MPAlP, (b) PBS/EDAP&MPAlP, and (c) PBS/EDAP&MPAlP/ZnB.

^{27}Al MAS NMR was used to analyze the transformation of aluminates upon heating (Figure 8). For PBS/MPAlP in 0 s, there are two signals at 39.3 ppm and 17.6 ppm (Figure 8a), which are

assigned to the presence of tetrahedrally coordinated AlO_4 ($AlPO_4$, coordinated with phosphate groups sharing the oxygen) and octahedrally coordinated AlO_6 (surrounded by phosphates, phosphorus atoms in their second sphere of coordination), respectively [51-53]. At 130 s, the signal intensity of AlO_6 increases and becomes dominant, indicating that parts of the AlO_4 are converted into AlO_6 under heat radiation and combustion [54]. Note that an additional band centered at 1.3 ppm appears when time exceeds 370s, indicating the formation of amorphous AlO_5 (no coordination to phosphate units, possibly a transition phase of conversion) during combustion [33] [55]. Besides, the broadening of the signal from 15 to -60 ppm evidences large distribution of Al surrounding assigned to the presence of amorphous network structures, which restricts the formation of well-ordered aluminophosphate frameworks.

The ^{27}Al NMR signals obviously change with the addition of EDAP (Figure 8b). At 130 s, the band of AlO_4 disappears for PBS/EDAP&MPAlP and the signal is dominated by a peak at -15.5 ppm (AlO_6). This is explained by the fact that most of AlO_4 is converted to AlO_6 and some aluminophosphates are formed as a result of chemical interaction between EDAP and MPAlP. Moreover, the shape of the AlO_6 signal is narrower when t >130 s, corresponding to the more ordered species, similar to crystalline structures. In the ^{27}Al NMR spectrum of PBS/EDAP&MPAlP/ZnB at 130 s (Figure 8c), there is an increased intensity of band at -17.6 ppm (the ratio of AlO_4/AlO_6 changes from 1:0.38 (t = 0 s) to 1:7.6 (t = 130 s)). However, when the combustion time exceeds 370s, the signal intensity of AlO_4 at around 38.6 ppm increases compared to that of AlO_6 (AlO_4/AlO_6 ratio of 1.58:1), which corresponds to the higher degree of condensation of the well-crystallized aluminophosphate network [51, 56].

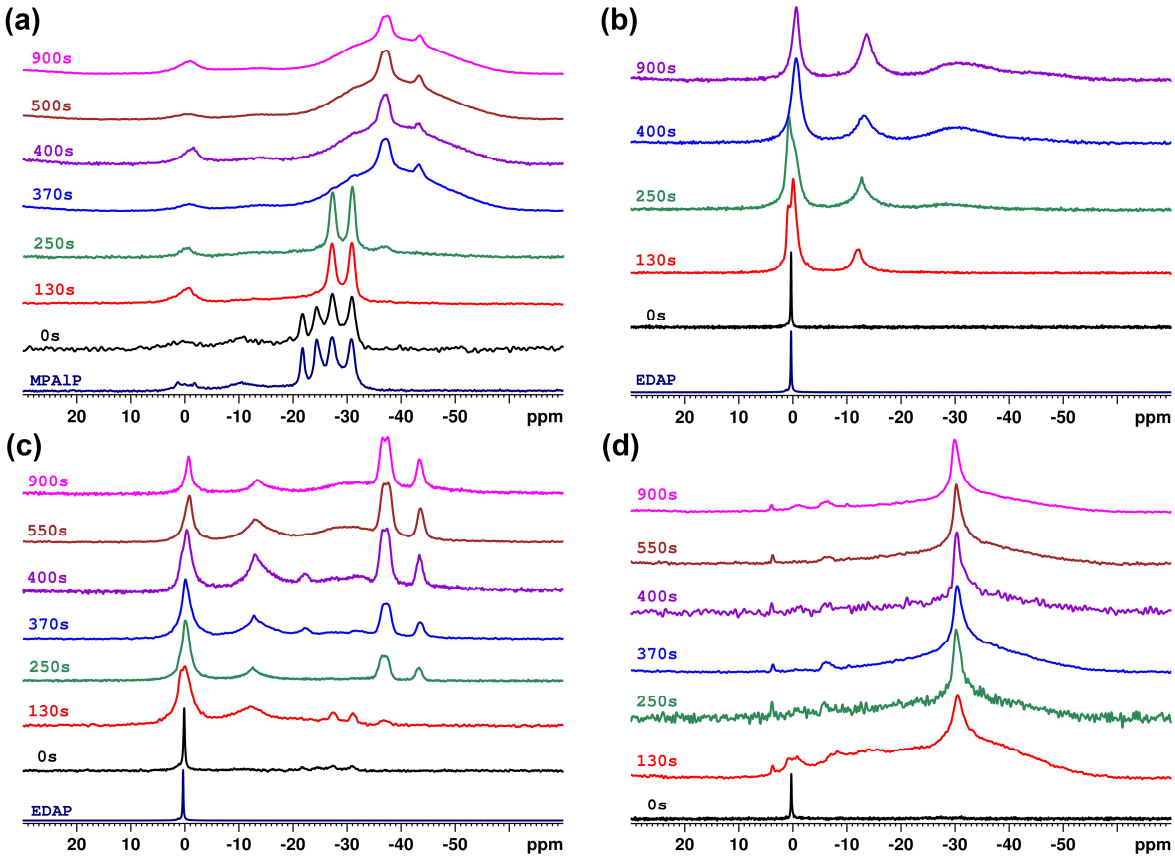

Figure 9. ^{31}P DD-MAS ssNMR spectra of (a) PBS/MPAlP, (b) PBS/EDAP, (c) PBS/EDAP&MPAlP, and (d) PBS/EDAP&MPAlP/ZnB.

In order to estimate the evolution of the phosphate species in the residues, the ^{31}P DD-MAS NMR spectra of PBS composites were studied (Figure 9). The peak position of ^{31}P NMR spectra depends on the phosphate structure, responding to the varying number of bridging oxygen atoms (Q^n, n refers to the number of bridging oxygen atoms per phosphate tetrahedron) [41]. The ^{31}P NMR spectrum of original MPAlP exhibits three sets of bands (Figure 9a). The low intense band at around 0 ppm is assigned to the trace amount of orthophosphate (Q^0). The band at -10.4 ppm is ascribed to terminal phosphate groups and/or pyrophosphate (Q^1). Besides, the doublet at -21.8 and -24.5 ppm are assigned to middle groups of polyphosphate chain (Q^2), which are widely found in polyphosphates [41]. Other doublet at -27.3 and -30.9 ppm are derived from $AlPO_4$ groups,

which is closer to proton source from melamine molecule, possibly connected by hydrogen bond [33]. In addition, ^{31}P NMR spectrum of EDAP (Figure 9b) exhibits a single peak at 0 ppm, which is ascribed to the characteristic of orthophosphates and/or phosphoric acid (Q^0) [28].

The ^{31}P spectrum of PBS/MPAlP at 0s shows signals similar to that of MPAlP, however, the doublet at -21.8 and -24.5 ppm (from the polyphosphate chain (Q^2) of MPAlP) disappears at 130 s, which was also observed in our previous works [33]. Besides, a broad signal between -20 and -60 ppm and two intense peaks (crystalline) at -37.3, -43.3 ppm are distinguished in 370 s, suggesting the presence of multiple species (amorphous and ordered structures), which is consistent with ^{27}Al NMR. The doublet of PBS/EDAP spectrum in 130 s is found at around -1 ppm, indicating the presence of orthophosphate bound to aliphatic species (Q^0 site, P-O-C links) [57]. Besides, an additional signal with low intensity at around -12 ppm is observed, which is contributed to pyrophosphates and/or orthophosphate linked to the aromatic species [41]. A broad band centered at around -30 ppm is detected from 250 s, corresponding to the formation of amorphous phosphate species exhibiting Q^3 site probably due to the condensation to ultraphosphate [58].

The ^{31}P NMR spectra of PBS/EDAP&MPAlP (Figure 9c) exhibit the combined signals of PBS/MPAlP and PBS/EDAP. The signals at -37.4, -43.4 ppm appears in 250 s, which is earlier than that of PBS/MPAlP (370 s), suggesting that the addition of EDAP promotes the decomposition of the composite. Interestingly, all bands are sharp when time exceeds 250 s, which confirms the formation of phosphorus-containing ordered structures embedded in the charred structure and thus improving the fire retardancy of char [59].

For the ^{31}P NMR spectra of PBS/EDAP&MPAlP/ZnB (Figure 9d), a broad resonance between 5 and -60 ppm is observed from 130 s, and this broad signal is still detected until 900 s. This

phenomenon implies that the addition of zinc borate yields some new species via chemical interactions, which may be contributed to the formation of a more stable char. Indeed, the broad resonance shows characteristic bands of the structure found in glass or amorphous compounds, while narrower signals are characteristic of ordered phases such as borophosphate, aluminophosphate, zinc phosphate/pyrophosphate/polyphosphate, and other phosphate glasses [37, 38]. For instance, the band at 3.9 ppm is assigned to zinc phosphate (α-$Zn_3(PO_4)_2$) [36] , whereas the intense signal at -30.2 ppm is assigned to borophosphate and/or aluminum phosphate [55].

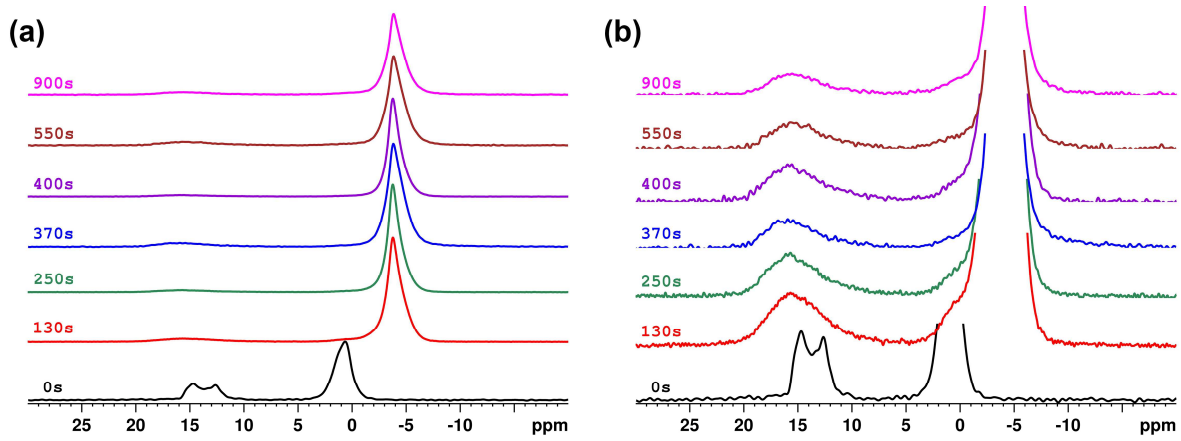

Figure 10. ^{11}B MAS ssNMR spectra of (a, b) PBS/EDAP&MPAlP/ZnB.

^{11}B MAS NMR spectra of PBS/EDAP&MPAlP/ZnB was further investigated to verify those conclusions (Figure 10). It is clearly seen that the spectrum of unburned sample (0s) exhibits a doublet centered at 14.6 and 12.6 ppm, which is ascribed to the BO_3 (trigonal borate) units [37]. Besides, another band located at 0.6 ppm is assigned to chemical shift of the BO_4 (tetragonal borate) units. With advancing burning process, the signal assigned to BO_3 units shifts to 15.7 ppm and shows a weak intensity; whereas the resonance of BO_4 units at 0.6 ppm shifts to -3.8 ppm corresponding to the presence of boron phosphate [60]. Note that a shoulder signal is also observed

at around 0 ppm, which is assigned to another type of borophosphate [37]. The result confirms unambiguously that borates react with phosphates upon heating to yield borophosphates, [61], which has been confirmed by the ^{31}P NMR results.

3.4 TGA and TGA-FTIR analyses

3.4.1 Thermal stability

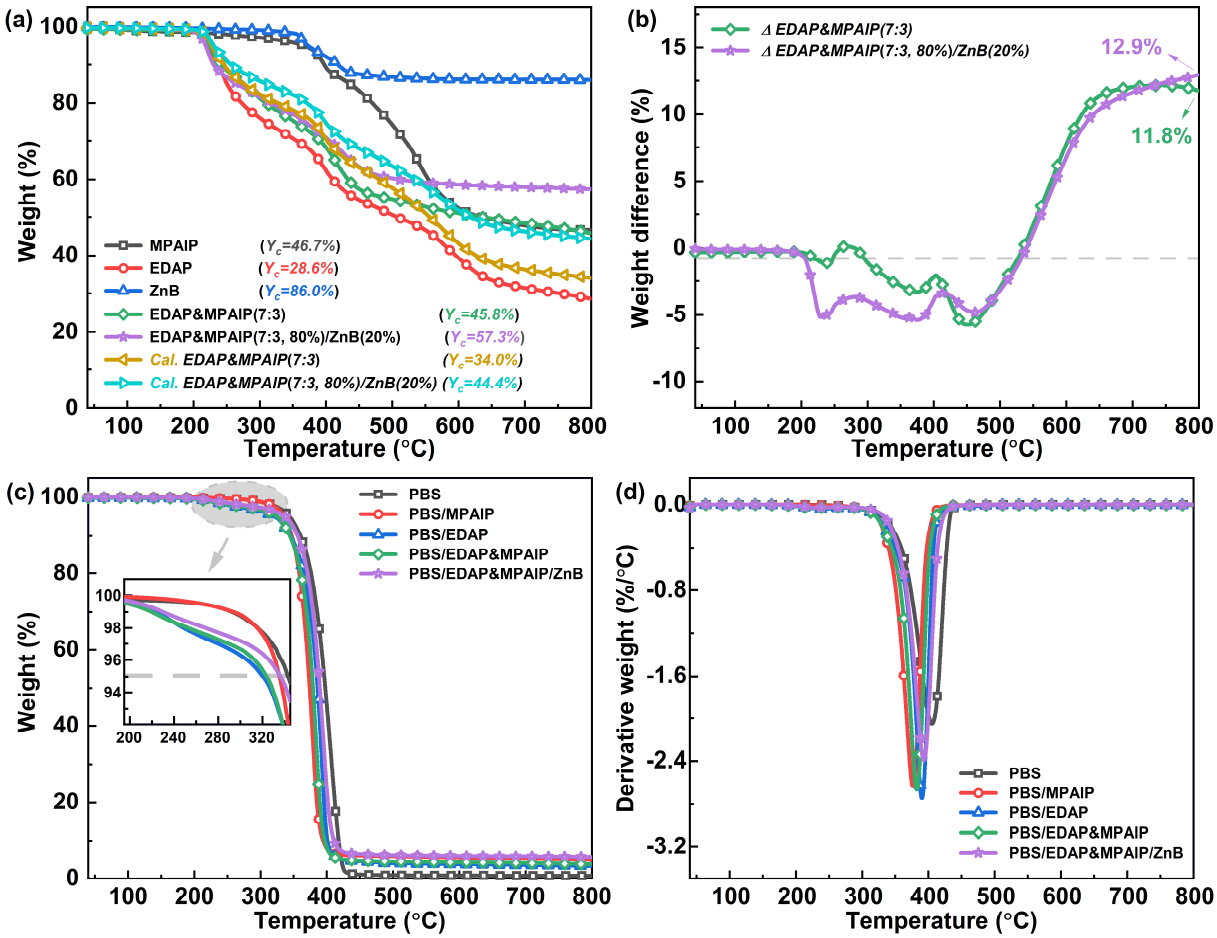

Figure 11. (a) TGA and (b) weight difference curves of additives and its mixtures under N_2 atmosphere; (c) TGA and (d) DTG curves of neat PBS and its composites under nitrogen atmosphere at a heating rate of 10 ºC/min.

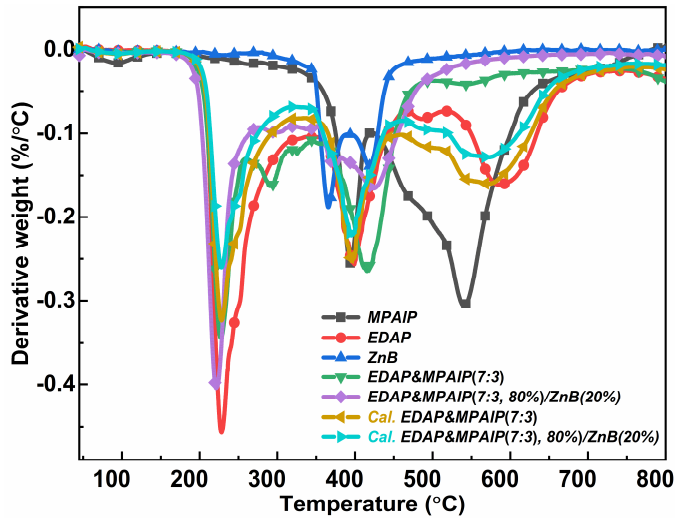

Figure S1. DTG curves of FR additives and their mixtures under N_2 atmosphere.

Table 4. TGA data of pure PBS and flame retarded PBS composites.

Sample	$T_{5\%}$ (ºC)	$T_{50\%}$ (ºC)	T_{max} (ºC)	Y_c (%) at 800 ºC
PBS	343	398	412	0.8
PBS/MPAlP	335	374	379	4.9
PBS/EDAP	320	386	392	3.3
PBS/EDAP&MPAlP	324	379	384	3.8
PBS/EDAP&MPAlP/ZnB	336	390	395	5.8

The thermal stabilities of additives and of their PBS composites were investigated to understand the effect of additives on the decomposition of PBS composites (Figure 11) [62]. MPAlP exhibits good thermal stability with two-stage thermal decompositions (350-420 ºC, 425-650 ºC, Figure S1) with a char yield of 46.7% at 800 ºC. Besides, decomposition in 3 steps is observed for EDAP (Figure S1), leaving 28.6% char residue at 800 ºC. The initial decomposition temperature ($T_{5\%}$, where 5 wt.% weight loss occurs)) of EDAP is around 225 ºC. The weight loss of zinc borate around 350-450 ºC involves the release of water and the condensation (B-OH groups) and crystallization processes of zinc borate [61]. In addition, it shows high thermal stability at 800 ºC with a residue of 86.0%. Moreover, the mass loss of mixtures (*i.e.*,

EDAP&MPAlP and EDAP&MPAlP/ZnB) occur in two main stages: the first stage in the temperature range 200-250 ºC (approximately 12% weight loss) corresponds to the decomposition of EDAP, releasing various gaseous products such as ammonia [31]; the second stage (between 370-470 ºC) is attributed to the decomposition of MPAlP and the chemical reaction between the additives. Note that the decomposition rates of EDAP&MPAlP and EDAP&MPAlP/ZnB are considerably slowed down between 480 and 800 ºC, indicating the formation of thermally stable species at an earlier stage.

In addition, weight difference curves allow pointing out a potential interaction and decrease or increase in the thermal stability of a combination of two or more ingredients when mixed together [44]. It can be seen that the weight differences of EDAP&MPAlP and EDAP&MPAlP/ZnB are negative ($\Delta<0$) in the temperature range of 200-540 ºC (Figure 11b), indicating the presence of chemical interaction between MPAlP and EDAP. Moreover, upon being heated to 540 ºC, the weight differences between the experimental and calculated curves increase progressively ($\Delta>0$), reaching 11.8% and 12.9% respectively at 800 ºC. This result suggests the fact that the interaction between MPAlP and EDAP enable a thermal stabilization of the residue at higher temperatures, which seems to be promising in terms of fire retardancy [57].

TGA and DTG curves of PBS and its composites in nitrogen are presented in Figure 11c-d, and relative data including initial degradation temperature ($T_{5\%}$), half degradation temperature ($T_{50\%}$, where 50 wt.% weight loss occurs), the temperature at maximum weight loss rate (T_{max}), and the yield of residual char (Y_c) are summarized in Table 4. Neat PBS decomposes from 343 ºC ($T_{5\%}$) in one-stage reaction under nitrogen atmosphere leaving almost no residue above 430 ºC. For all flame retarded PBS formulations, the addition of additives in PBS slightly decreases the $T_{5\%}$, $T_{50\%}$, and T_{max} of composites. This is due to the incorporation of flame retardants catalyzed

the decomposition of PBS. It is worth noting that EDAP-containing PBS composites show two degradation stages, the first stage is contributed to the earlier degradation of EDAP, which results in approximately 4% mass loss of composites. With the incorporation of 10 wt.% EDAP, the $T_{5\%}$ of PBS/EDAP decreases from 343 ºC to 320 ºC. Partial substitution of EDAP&MPAlP by 2 wt.% zinc borate shows a positive effect on the thermal stability of PBS/EDAP&MPAlP/ZnB in comparison with PBS/EDAP&MPAlP (the $T_{5\%}$, $T_{50\%}$, and T_{max} increase by 12 ºC, 11 ºC, and 11 ºC, respectively). Meanwhile, the addition of zinc borate leads to a higher Y_c (5.8% vs. 3.8%). These observations are presumably ascribed to a thermal stabilization effect of the residual char by the zinc borate at higher temperatures.

3.4.2 TGA-FTIR analysis

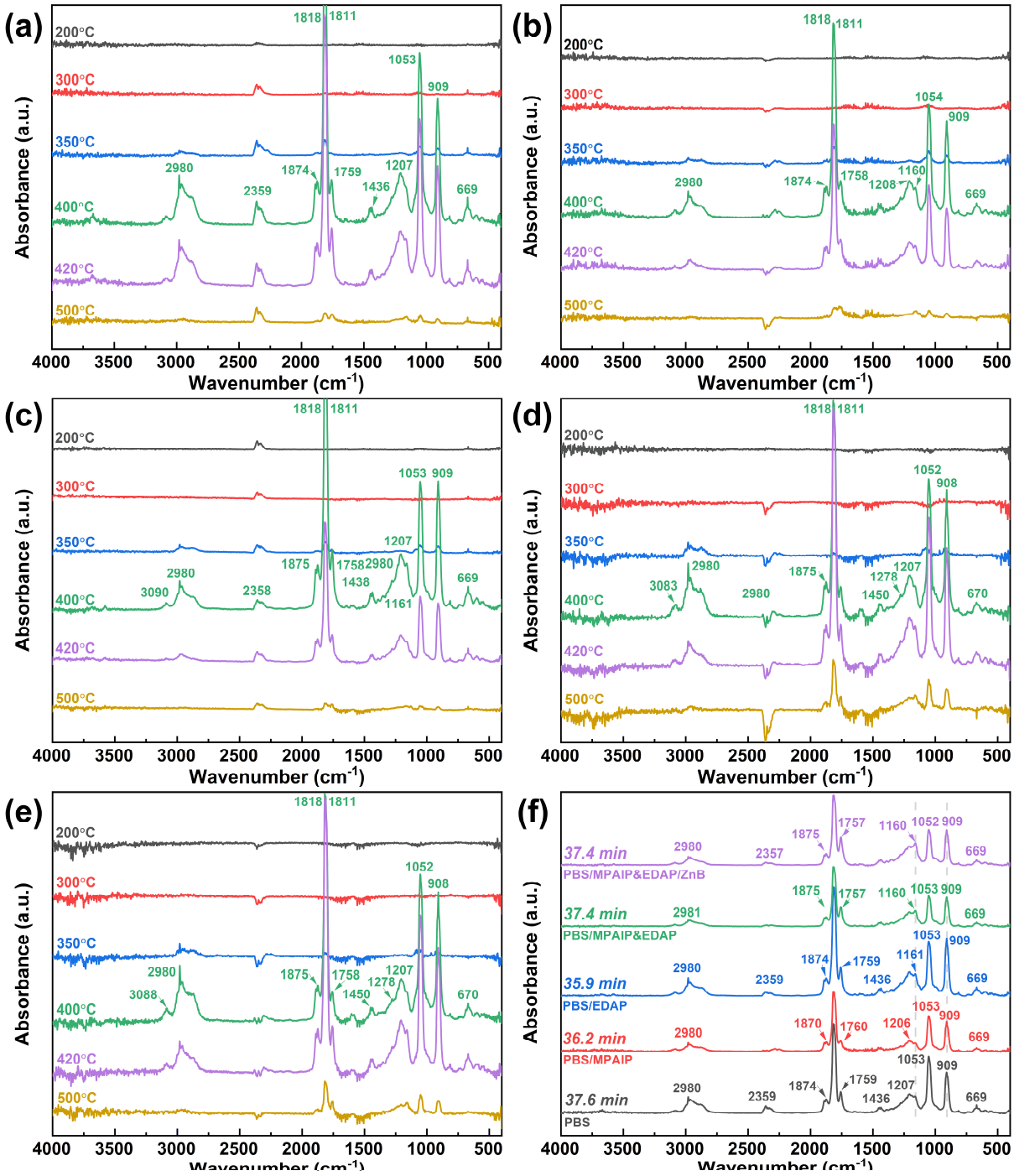

Figure 12. TGA-FTIR absorbance spectra of pyrolysis gases for (a) PBS, (b) PBS/MPAlP, (c) PBS/EDAP, (d) PBS/EDAP&MPAlP, and (e) PBS/EDAP&MPAlP/ZnB; and (f) FTIR absorbance spectra of pyrolysis gases for neat PBS and its composites at the maximum evolution rate.

TGA-FTIR were used to investigate the decomposition products of PBS and its composites under nitrogen atmosphere. As presented in Figure 12a, PBS shows strong characteristic FTIR bands at around 3000-3100 cm^{-1} (unsaturated alkane), 2800-3000 cm^{-1} (hydrocarbons), 2300-2400 cm^{-1} (carbon dioxide), 1811-1818 cm^{-1} (carbonyl compounds), 1100-1250 cm^{-1} (aliphatic ethers) [7]. The FTIR spectra of pyrolysis gases for PBS composites (Figure 12b-e) at different times show similar characteristic absorption bands to neat PBS. It is speculated that some characteristic absorption bands produced by the decomposition of flame retardants may overlap with the absorption bands of the PBS matrix[17]. On the other hand, the low additive loading (10 wt.%) may cause the decreased absorption intensity of characteristic peaks.

The FTIR absorbance spectra of pyrolysis gases for PBS and its composites at the maximum evolution rate were investigated (Figure 12f). Compared to neat PBS, the absorption intensities of PBS composites at 909 cm^{-1} significantly enhance when incorporating MPAlP and/or EDAP into PBS. This phenomenon is due to the absorption band of C-H (deformation vibration of alkene) is overlapped by the additional absorption of ammonia decomposed from MPAlP and EDAP [16]. The evolved ammonia can provide a gas phase action during combustion through a fuel dilution effect [63]. The maximum decomposition rates of PBS, PBS/MPAlP, PBS/EDAP, PBS/EDAP&MPAlP, and PBS/EDAP&MPAlP/ZnB occur at 37.6 min (413 ℃), 36.2 min (399 ℃), 35.9 min (396 ℃), 37.4 min (411 ℃), 37.4 min (411 ℃), respectively. This means that the addition of MPAlP and/or EDAP promotes the thermal decomposition of PBS matrix and catalyzes the formation of residue.

3.5 Flame retardant mechanisms

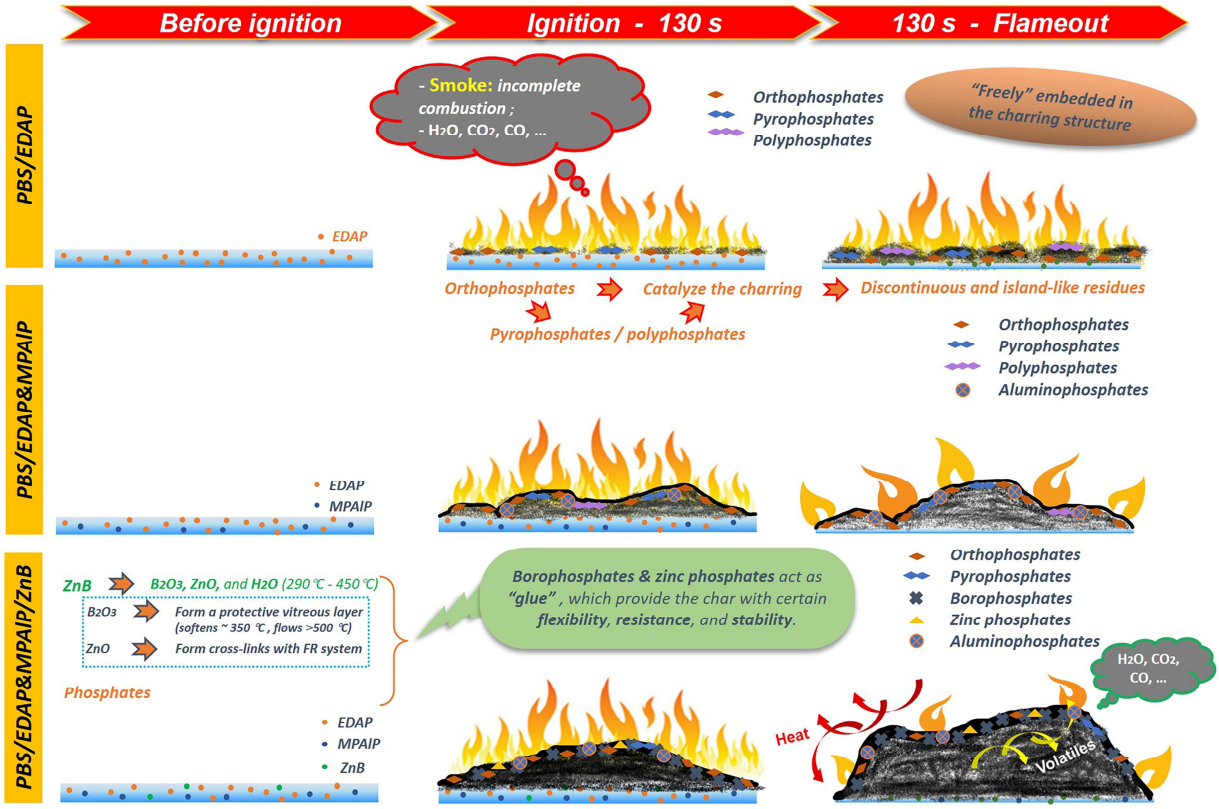

Figure 13. Flame-retardant mechanism for PBS composites.

From the above discussion, the mechanism of flame-retardant actions of PBS composites is proposed in Figure 13. Upon heating, flame retarded PBS formulations decompose and produce char residue. For PBS/MPAlP, amorphous aluminophosphate species are produced in the char during combustion. However, the formed char is not strong enough to provide adequate protection to the underneath polymer matrix, thus resulting in poor fire performance. The incorporation of EDAP alone leads to the formation of only "free" condensed phosphates embedded in the charring structure, which cannot effectively improve the fire performance of char. Moreover, the combination of MPAlP and EDAP leads to the formation of an intumescent charring structure embedded with aluminophosphate species, which provides the char with certain flexibility and

stability. However, the resultant char is not strong enough to resist the heat flux and fire, which results in the appearance of holes and cracks on the surface of char, thereby presenting a limited enhancement of flame retardancy in terms of pHRR.

It is proved unambiguously that, for PBS/EDAP&MPAlP/ZnB, the presence of zinc borate promotes the formation of thermally stable inorganic phosphate species (borophosphates, zinc phosphates, and aluminophosphates), which reinforces the char structure and provides an additional fire barrier to the char with good flexibility and cohesion. The formed protective crack-free intumescent char effectively limits the mass (fuel) and heat transfer between condensed and gas phases, thus improving the fire retardancy of PBS.

3.6 Mechanical performance

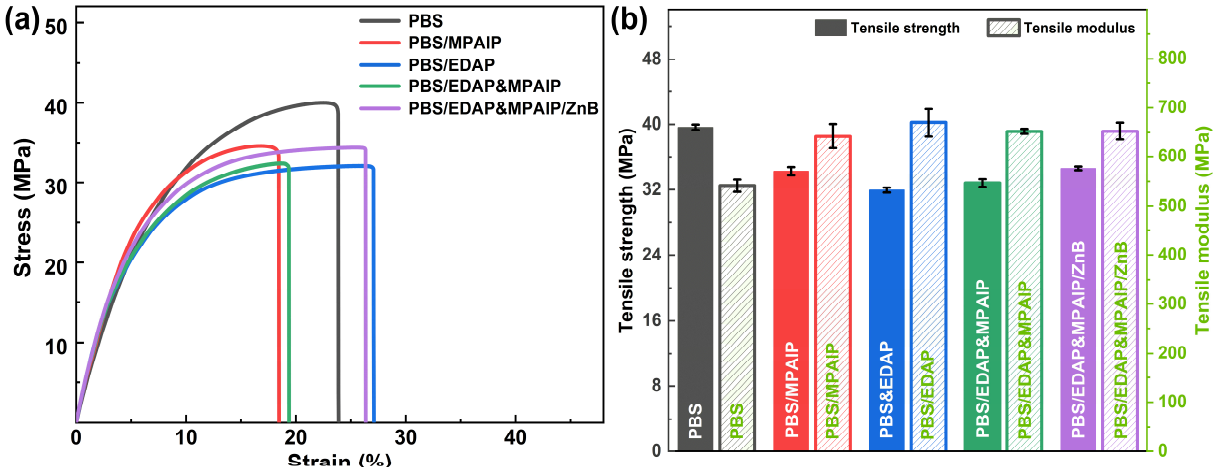

Figure 14. (a-b) Stress-strain curves of PBS and its composites.

Tensile test of PBS and its composites was performed to study the effect of the additives on the mechanical properties of PBS. The tensile strengths of PBS, PBS/MPAlP, PBS/EDAP, PBS/EDAP&MPAlP, and PBS/EDAP&MPAlP/ZnB composites are 39.7, 34.3, 32.0, 32.8, and 34.6 MPa, respectively (Figure 14). It is observed that neat PBS shows higher tensile strength than

all flame retarded PBS composites. The decrease of tensile strength of PBS composites is ascribed to the poor compatibility between the flame-retardant additives and PBS matrix. Indeed, similar conclusions have been widely demonstrated in other intumescent flame retardant systems that the incorporation of intumescent flame-retardant additives into polymer or polymer composite at a relatively high loading can cause a negative impact on the mechanical properties of polymer matrix [19, 64]. The presence of 10 wt.% MPAlP in PBS causes a decrease of tensile strength by 13.6% in comparison with that of neat PBS. When adding 10 wt.% of EDAP to PBS, the tensile strength of PBS/EDAP is reduced by 19.4% from 39.7 MPa for neat PBS to 32.0 MPa. Besides, the combination of EDAP and MPAlP slightly increases the tensile strength of PBS when compared with that of PBS/EDAP formulation, which may be due to the better interfacial interaction between PBS and MPAlP. It is worth noting that, compared to PBS/EDAP&MPAlP, a reinforcement effect is observed when zinc borate is incorporated.

The tensile modulus of PBS formulations is also presented in Figure 14b. On the contrary to the tensile strength, the introduction of additives increases the tensile modulus of PBS. The tensile modulus of PBS/MPAlP, PBS/EDAP, PBS/EDAP&MPAlP, and PBS/EDAP&MPAlP/ZnB composites are 642, 670, 652, and 653 MPa, respectively, which are higher than that of unfilled PBS. The results show that the incorporation of flame retardants does not cause a drastic decrease in the mechanical properties of the PBS, which exhibits acceptable mechanical properties.

4. Conclusions

In summary, we reported a new intumescent flame retardant system for PBS with high fire protection efficiency via incorporating MPAlP and EDAP as well as zinc borate. The combination of intumescent additives at a relatively low content (10 wt.%) in PBS permitted the reductions of pHRR and of THR by 63% and 13% respectively. Besides, the FIGRA and MARHE of

PBS/EDAP&MPAlP/ZnB composite were markedly reduced by 43 and 48% respectively, and the FRI value reached 3.13. It was confirmed that a condensed phase flame retardant mechanism was established through the formation of a protective intumescent char layer during combustion. This formed intumescent char effectively retarded the transfer of heat and mass (fuel) between condensed and gas phases. Further, the MAS NMR analyses exhibited that the introduction of zinc borate promoted the formation of a protective intumescent char embedded with highly thermally stable inorganic phosphate species, which provided additional cohesion and stability to the char, thus enhancing the flame retardancy of material. Moreover, with the addition of zinc borate, PBS/EDAP&MPAlP/ZnB showed low smoke emission and good mechanical/thermal properties.

Acknowledgements

The authors would like to acknowledge Johan Sarazin and Adeline Marin for their guidance on measurements, and we are especially grateful to Bertrand Doumert and Bertrand Revel for recording solid-state NMR spectra. In addition, Fei Xiao is supported by the scholarship from the China Scholarship Council (*No. 201804910605*).

References

[1] L. Liu, G. Huang, P. Song, Y. Yu, S. Fu, Converting industrial alkali lignin to biobased functional additives for improving fire behavior and smoke suppression of polybutylene succinate, ACS Sustain. Chem. Eng. 4(9) (2016) 4732-4742.

[2] T. Kuang, J. Ju, Z. Yang, L. Geng, X. Peng, A facile approach towards fabrication of lightweight biodegradable poly (butylene succinate)/carbon fiber composite foams with high electrical conductivity and strength, Compos. Sci. Technol. 159 (2018) 171-179.

[3] Z. Lule, J. Kim, Surface modification of aluminum nitride to fabricate thermally conductive poly (butylene succinate) nanocomposite, Polymers 11(1) (2019) 148.

[4] H. Chen, T. Wang, Y. Wen, X. Wen, D. Gao, R. Yu, X. Chen, E. Mijowska, T. Tang, Expanded graphite assistant construction of gradient-structured char layer in PBS/Mg (OH) 2 composites for improving flame retardancy, thermal stability and mechanical properties, Compos. B. Eng. 177 (2019) 107402.

[5] G. Dorez, A. Taguet, L. Ferry, J.M.L. Cuesta, Phosphorous compounds as flame retardants for polybutylene succinate/flax biocomposite: Additive versus reactive route, Polym. Degrad. Stab. 102 (2014) 152-159.

[6] H. Yang, B. Yu, X. Xu, S. Bourbigot, H. Wang, P. Song, Lignin-derived bio-based flame retardants toward high-performance sustainable polymeric materials, Green Chemistry 22(7) (2020) 2129-2161.

[7] X. Wang, Y. Hu, L. Song, H. Yang, B. Yu, B. Kandola, D. Deli, Comparative study on the synergistic effect of POSS and graphene with melamine phosphate on the flame retardance of poly(butylene succinate), Thermochim. Acta 543 (2012) 156-164.

[8] L. Ferry, G. Dorez, A. Taguet, B. Otazaghine, J.M. Lopez-Cuesta, Chemical modification of lignin by phosphorus molecules to improve the fire behavior of polybutylene succinate, Polym. Degrad. Stab. 113 (2015) 135-143.

[9] H. Yang, L. Song, Q. Tai, X. Wang, B. Yu, Y. Yuan, Y. Hu, R.K.K. Yuen, Comparative study on the flame retarded efficiency of melamine phosphate, melamine phosphite and melamine hypophosphite on poly(butylene succinate) composites, Polym. Degrad. Stab. 105 (2014) 248-256.

[10] C. Hu, S. Bourbigot, T. Delaunay, M. Collinet, S. Marcille, G. Fontaine, Synthesis of isosorbide based flame retardants: Application for polybutylene succinate, Polym. Degrad. Stab. 164 (2019) 9-17.

[11] W. He, P. Song, B. Yu, Z. Fang, H. Wang, Flame retardant polymeric nanocomposites through the combination of nanomaterials and conventional flame retardants, Prog. Mater Sci. 114 (2020) 100687.

[12] F. Xiao, G. Fontaine, S. Bourbigot, Recent developments in fire retardancy of polybutylene succinate, Polym. Degrad. Stab. 183 (2021) 109466.

[13] J. Alongi, Z. Han, S. Bourbigot, Intumescence: Tradition versus novelty. A comprehensive review, Prog. Polym. Sci. 51 (2015) 28-73.

[14] S. Bourbigot, M. Le Bras, S. Duquesne, M. Rochery, Recent advances for intumescent polymers, Macromolecular Materials and Engineering 289(6) (2004) 499-511.

[15] X. Yue, J. Li, P. Liu, W. Pu, Y. Lin, Investigation of flame-retarded poly(butylene succinate) composites using MHSH as synergistic and reinforced agent, J. Mater. Sci. 53(7) (2017) 5004-5015.

[16] Y. Chen, J. Zhan, P. Zhang, S. Nie, H. Lu, L. Song, Y. Hu, Preparation of intumescent flame retardant poly (butylene succinate) using fumed silica as synergistic agent, Industrial & Engineering Chemistry Research 49(17) (2010) 8200-8208.
[17] X. Wang, L. Song, H. Yang, H. Lu, Y. Hu, Synergistic effect of graphene on antidripping and fire resistance of intumescent flame retardant poly(butylene succinate) composites, Industrial & Engineering Chemistry Research 50(9) (2011) 5376-5383.
[18] Y. Wang, S. Zhang, X. Wu, C. Lu, Y. Cai, L. Ma, G. Shi, L. Yang, Effect of montmorillonite on the flame-resistant and mechanical properties of intumescent flame-retardant poly(butylene succinate) composites, J. Therm. Anal. Calorim. 128(3) (2017) 1417-1427.
[19] Y. Wang, C. Liu, X. Shi, J. Liang, Z. Jia, G. Shi, Synergistic effect of halloysite nanotubes on flame resistance of intumescent flame retardant poly (butylene succinate) composites, Polym. Compos. 40(1) (2019) 202-209.
[20] C. Hu, Flame retardancy of polybutylene succinate by multiple approaches, University of Lille, 2018.
[21] P. Liu, X. Yue, G. He, X. Zhang, Y. Sun, Influence of modified fiber–MHSH hybrids on fire hazards, combustion dynamics, and mechanical properties of flame-retarded poly(butylene succinate) composites, J. Appl. Polym. Sci. 137(12) (2019) 48490.
[22] L. Gu, S. Zhang, H. Li, J. Sun, W. Tang, L. Zhao, X. Gu, Preparation of Intumescent Flame Retardant Poly (butylene succinate) Using Urea Intercalated Kaolinite as Synergistic Agent, Fibers and Polymers 20(8) (2019) 1631-1640.
[23] S. Zhang, Y. Li, J. Guo, L. Gu, H. Li, B. Fei, J. Sun, X. Gu, Preparation of hexakis (4-aldehyde phenoxy) cyclotriphosphazene grafted kaolinite and its synergistic fire resistance in poly (butylene succinate), Polym. Compos. 41(3) (2020) 1024-1035.
[24] X. Yue, Y. Li, J. Li, Y. Xu, Improving fire behavior and smoke suppression of flame-retardant PBS composites using lignin chelate as carbonization agent and catalyst, J. Appl. Polym. Sci. (2021) 51199.
[25] X. Yue, C. Li, Y. Li, Using colloidal lignin intercalated montmorillonite nanosheets as synergistic and reinforced agent for flame-retardant poly (butylene succinate) composites, Polym. Adv. Technol.
[26] Y.-J. Liu, L. Mao, S.-h. Fan, Preparation and study of intumescent flame retardant poly(butylene succinate) using MgAlZnFe-CO3layered double hydroxide as a synergistic agent, J. Appl. Polym. Sci. 131(17) (2014) 40736.
[27] L. Dumazert, D. Rasselet, B. Pang, B. Gallard, S. Kennouche, J.-M. Lopez-Cuesta, Thermal stability and fire reaction of poly(butylene succinate) nanocomposites using natural clays and FR additives, Polym. Adv. Technol. 29(1) (2018) 69-83.
[28] F. Xiao, G. Fontaine, S. Bourbigot, Intumescent polybutylene succinate : ethylenediamine phosphate and synergists, Polym. Degrad. Stab. (2021) 109707.
[29] A. Sut, E. Metzsch-Zilligen, M. Großhauser, R. Pfaendner, B. Schartel, Synergy between melamine cyanurate, melamine polyphosphate and aluminum diethylphosphinate in flame retarded thermoplastic polyurethane, Polym. Test. 74 (2019) 196-204.
[30] J. Davis, M. Huggard, The technology of halogen-free flame retardant phosphorus additives for polymeric systems, Journal of Vinyl and Additive Technology 2(1) (1996) 69-75.

[31] H.J. Kruger, W.W. Focke, W. Mhike, A. Taute, A. Roberson, Thermal properties of polyethylene flame retarded with expandable graphite and intumescent fire retardant additives, Fire and Materials 41(6) (2017) 573-586.
[32] A.D. Naik, G. Fontaine, F. Samyn, X. Delva, Y. Bourgeois, S. Bourbigot, Melamine integrated metal phosphates as non-halogenated flame retardants: Synergism with aluminium phosphinate for flame retardancy in glass fiber reinforced polyamide 66, Polym. Degrad. Stab. 98(12) (2013) 2653-2662.
[33] A.D. Naik, G. Fontaine, F. Samyn, X. Delva, J. Louisy, S. Bellayer, Y. Bourgeois, S. Bourbigot, Mapping the multimodal action of melamine-poly(aluminium phosphate) in the flame retardancy of polyamide 66, RSC Adv. 4(35) (2014) 18406-18418.
[34] A.D. Naik, G. Fontaine, F. Samyn, X. Delva, J. Louisy, S. Bellayer, Y. Bourgeois, S. Bourbigot, Outlining the mechanism of flame retardancy in polyamide 66 blended with melamine-poly(zinc phosphate), Fire Safety J 70 (2014) 46-60.
[35] P. Müller, B. Schartel, Melamine poly(metal phosphates) as flame retardant in epoxy resin: Performance, modes of action, and synergy, J. Appl. Polym. Sci. 133(24) (2016) 43549.
[36] P. Müller, M. Morys, A. Sut, C. Jäger, B. Illerhaus, B. Schartel, Melamine poly(zinc phosphate) as flame retardant in epoxy resin: Decomposition pathways, molecular mechanisms and morphology of fire residues, Polym. Degrad. Stab. 130 (2016) 307-319.
[37] S. Bourbigot, J. Sarazin, T. Bensabath, Intumescent polypropylene in extreme fire conditions, Fire Safety J (2020) 103082.
[38] F. Samyn, S. Bourbigot, S. Duquesne, R. Delobel, Effect of zinc borate on the thermal degradation of ammonium polyphosphate, Thermochim. Acta 456(2) (2007) 134-144.
[39] M.A. Oualha, N. Amdouni, F. Laoutid, Synergistic flame-retardant effect between calcium hydroxide and zinc borate in ethylene-vinyl acetate copolymer (EVA), Polym. Degrad. Stab. 144 (2017) 315-324.
[40] S. Yang, G. Lv, Y. Liu, Q. Wang, Synergism of polysiloxane and zinc borate flame retardant polycarbonate, Polym. Degrad. Stab. 98(12) (2013) 2795-2800.
[41] S. Bourbigot, J. Sarazin, F. Samyn, M. Jimenez, Intumescent ethylene-vinyl acetate copolymer: Reaction to fire and mechanistic aspects, Polym. Degrad. Stab. 161 (2019) 235-244.
[42] C. Hoffendahl, G. Fontaine, S. Duquesne, F. Taschner, M. Mezger, S. Bourbigot, The fire retardant mechanism of ethylene vinyl acetate elastomer (EVM) containing aluminium trihydroxide and melamine phosphate, RSC Advances 4(39) (2014) 20185-20199.
[43] B. Prieur, M. Meub, M. Wittemann, R. Klein, S. Bellayer, G. Fontaine, S. Bourbigot, Phosphorylation of lignin to flame retard acrylonitrile butadiene styrene (ABS), Polym. Degrad. Stab. 127 (2016) 32-43.
[44] G. Fontaine, S. Bourbigot, Intumescent polylactide: a nonflammable material, J. Appl. Polym. Sci. 113(6) (2009) 3860-3865.
[45] B. Sundström, The development of a European fire classification system for building products-test methods and mathematical modelling, Lund University, 2007.
[46] H. Vahabi, B.K. Kandola, M.R. Saeb, Flame retardancy index for thermoplastic composites, Polymers 11(3) (2019) 407.

[47] W.-H. Rao, W. Liao, H. Wang, H.-B. Zhao, Y.-Z. Wang, Flame-retardant and smoke-suppressant flexible polyurethane foams based on reactive phosphorus-containing polyol and expandable graphite, J. Hazard. Mater. 360 (2018) 651-660.

[48] F. Ngohang, G. Fontaine, L. Gay, S. Bourbigot, Revisited investigation of fire behavior of ethylene vinyl acetate/aluminum trihydroxide using a combination of mass loss cone, Fourier transform infrared spectroscopy and electrical low pressure impactor, Polym. Degrad. Stab. 106 (2014) 26-35.

[49] X. Zhao, D. Xiao, J.P. Alonso, D.-Y. Wang, Inclusion complex between beta-cyclodextrin and phenylphosphonicdiamide as novel bio-based flame retardant to epoxy: Inclusion behavior, characterization and flammability, Materials & Design 114 (2017) 623-632.

[50] C. Hu, S. Bourbigot, T. Delaunay, M. Collinet, S. Marcille, G. Fontaine, Poly(isosorbide carbonate): A 'green' char forming agent in polybutylene succinate intumescent formulation, Compos. B. Eng. 184 (2020) 107675.

[51] U. Braun, B. Schartel, M.A. Fichera, C. Jäger, Flame retardancy mechanisms of aluminium phosphinate in combination with melamine polyphosphate and zinc borate in glass-fibre reinforced polyamide 6, 6, Polym. Degrad. Stab. 92(8) (2007) 1528-1545.

[52] J. Sarazin, C.A. Davy, S. Bourbigot, G. Tricot, J. Hosdez, D. Lambertin, G. Fontaine, Flame resistance of geopolymer foam coatings for the fire protection of steel, Compos. B. Eng. 222 (2021) 109045.

[53] A. Sut, S. Greiser, C. Jäger, B. Schartel, Synergy in flame-retarded epoxy resin, J. Therm. Anal. Calorim. 128(1) (2017) 141-153.

[54] L. Baggetto, V. Sarou-Kanian, P. Florian, A. Gleizes, D. Massiot, C. Vahlas, Atomic scale structure of amorphous aluminum oxyhydroxide, oxide and oxycarbide films probed by very high field 27 Al nuclear magnetic resonance, Physical Chemistry Chemical Physics 19(11) (2017) 8101-8110.

[55] A. Sut, S. Greiser, C. Jäger, B. Schartel, Interactions in multicomponent flame-retardant polymers: Solid-state NMR identifying the chemistry behind it, Polym. Degrad. Stab. 121 (2015) 116-125.

[56] F. Samyn, S. Bourbigot, Thermal decomposition of flame retarded formulations PA6/aluminum phosphinate/melamine polyphosphate/organomodified clay: interactions between the constituents?, Polym. Degrad. Stab. 97(11) (2012) 2217-2230.

[57] B. Lecouvet, M. Sclavons, C. Bailly, S. Bourbigot, A comprehensive study of the synergistic flame retardant mechanisms of halloysite in intumescent polypropylene, Polym. Degrad. Stab. 98(11) (2013) 2268-2281.

[58] C. Mercier, L. Montagne, H. Sfihi, G. Palavit, J.C. Boivin, A.P. Legrand, Local structure of zinc ultraphosphate glasses containing large amount of hydroxyl groups: 31P and 1H solid state nuclear magnetic resonance investigation, J. Non-Cryst. Solids 224(2) (1998) 163-172.

[59] S. Bourbigot, M. Le Bras, R. Delobel, R. Decressain, J.-P. Amoureux, Synergistic effect of zeolite in an intumescence process: study of the carbonaceous structures using solid-state NMR, J. Chem. Soc., Faraday Trans. 92(1) (1996) 149-158.

[60] A. Karrasch, E. Wawrzyn, B. Schartel, C. Jäger, Solid-state NMR on thermal and fire residues of bisphenol A polycarbonate/silicone acrylate rubber/bisphenol A bis (diphenyl-phosphate)/(PC/SiR/BDP) and PC/SiR/BDP/zinc

borate (PC/SiR/BDP/ZnB)–Part I: PC charring and the impact of BDP and ZnB, Polym. Degrad. Stab. 95(12) (2010) 2525-2533.
[61] Q.F. Gillani, F. Ahmad, M.I. Abdul Mutalib, P.S.M. Megat-Yusoff, S. Ullah, P.J. Messet, M. Zia-ul-Mustafa, Thermal degradation and pyrolysis analysis of zinc borate reinforced intumescent fire retardant coatings, Prog. Org. Coat. 123 (2018) 82-98.
[62] Y. He, H. Li, F. Luo, Y. Jin, B. Huang, Q. Qian, Bio-based flexible phase change composite film with high thermal conductivity for thermal energy storage, Compos. Part A Appl. Sci. Manuf. 151 (2021) 106638.
[63] S. Yang, S. Huo, J. Wang, B. Zhang, J. Wang, S. Ran, Z. Fang, P. Song, H. Wang, A highly fire-safe and smoke-suppressive single-component epoxy resin with switchable curing temperature and rapid curing rate, Compos. B. Eng. 207 (2021) 108601.
[64] N. Suppakarn, K. Jarukumjorn, Mechanical properties and flammability of sisal/PP composites: effect of flame retardant type and content, Compos. B. Eng. 40(7) (2009) 613-618.